A STRUCTURAL REVIEW OF THE PERFORMANCE OF CONCRETE PAVEMENTS PART 1

FLORIDA
DEPARTMENT OF TRANSPORTATION

FEBRUARY 10, 1986

Florida Department of Transportation

A STRUCTURAL REVIEW OF THE PERFORMANCE OF CONCRETE PAVEMENTS PART I

by
Paul F. Csagoly
Chief Structures Analyst

Tallahassee, Florida
February 10, 1986

ABSTRACT

Closed format and finite difference solutions to the fundamental partial differential equation, by which the interaction between a rigid pavement segment plate and the elastic subgrade is mathematically described, are presented in this report. The solutions permit a precise analysis of both separate and combined effects of dead weight, temperature and axle loads.

It has been found that extreme temperature effects may exceed the stresses due to heavy commercial vehicles by a factor of two. It is indicated that even the best pavement design is only marginal in terms of structural engineering and that an unfortunate combination of parameters, like the I-75 design, can surely lead to early deterioration. Sudden cooling by the environment or intensive rainfall may cause partial separation of the pavement from the subgrade and, if the subgrade is impervious, result in excessive pumping.

There appears to be no hope in designing a well performing pavement without an appropriate consideration for temperature. Accordingly, the AASHTO design process, which lacks such provision, should be revised considerably for future use in the State of Florida. It can also be demonstrated that the standard methods of testing, by which deflections are measured under static loads or falling weights, are insensitive to temperature and these methods need be altered and/or extended.

Acknowledgement

The author is indebted to William N. Nickas, structures analyst, for writing the computer programs and carrying out the computations in conjunction with the relaxation method of analysis applied, to Henry T. Bollmann, chief of Structures Design Bureau for allowing the author to work on this subject which until now has not been considered a structural one, and last but not least to Nedra Hill for typing the difficult text on the word processor.

Disclaimer

The conclusions drawn herein are those of the author and do not constitute either an adopted point of view or an official policy of the Florida Department of Transportation.

The author is prepared to take full responsibility-for the mathematical derivations obtained, but not for the physical database, which had been developed by and adopted from others.

Reference to the report is not opposed, however, in order to avoid out-of-context quotations, consultation with the author is recommended.

* Part II of this report will present the results of a two dimensional analysis of the concrete segments.

Content

List of Figures

1. Introduction

The author has been requested to review the structural behavior of concrete pavements, with particular reference to the unsatisfactory performance of a 29.1-mile section of I-75 in Sarasota and Manatee Counties, Florida. This relatively young section of pavement, which is supposed to have been designed to the best standards available, shows an extensive amount of undesirable cracking that cannot be explained by current methods of analysis and/or conventional speculation.

This report will demonstrate, in engineering terms, that sudden changes in temperature of the environment may substantially alter the nature of relationship between the subgrade and the concrete slab, causing tensile stresses in the concrete it cannot sustain. The separation between the subgrade and the slab, in the presence of free water, may lead to turbulent flow, migration of particles, and the collapse of the structural system under vehicular loads. It will be shown that the impervious and rigid subgrade in combination with the length and shape of the segments selected for the I-75 pavement produces an unsatisfactory design.

The idea of the 18 Kip axle weight equivalency may or may not work for flexible pavements, but it is demonstratively alien to the way rigid pavements perform. These pavements are exposed to relatively low levels of stress at which, the structural behavior is completely elastic, consequently, they can be analyzed by structural methods.

It will be illustrated that the basic Lagrange differential equation, by which the behavior of elastic plates is studied, can be extended to incorporate variable subgrade characteristics, the effect of temperature in addition to various boundary conditions of and interaction among the segments. A powerful method of relaxation in combination with present computer technology enables the structural engineer to analyze rigid pavement systems, no matter how complex they are.

For these computations, and for the verification of their outcome, a number of physical tests, other than the presently exclusive deflection test, will need be devised and carried out. These may include topics like thermal conductivity, specific heat, and change in temperature, solar radiation, subgrade shakedown, large plate "k" value, and turbulent flow through granular, lateral confinement and concrete tensile strength. With all that, an appropriate method of designing rigid pavements may emerge in the future.

2. I-75 Pavement Design

The nine inch thick concrete pavement is subdivided into randomly sequenced sections of 16.0, 17.0, 22.0, and 23.0 ft lengths. The 12.0-foot wide segments are, joined at a skew angle of 1:6. The election of the random lengths and skew was supposed to improve the riding quality of the surface.

There are three lanes in both South and North directions. The shoulders are also paved with econocrete. The longitudinal joints between the segments are keyed and tied with bars, the transverse joints are fitted out with dowels of standard design.

The pavement is supported by a 6 inch thick econocrete subgrade, which is 40.0 feet wide. Bond between the econocrete subgrade and spraying the econocrete with a curing compound, into which wax was mixed, had prevented the concrete pavement. From the engineering point of view, the pavement consists of two non-composite concrete plates.

Some years ago, FDOT constructed several test areas of various pavement designs on U.S. 41, North of Ft. Myers. At least one area incorporated econocrete as subbase, but it featured a rectangular pattern of subdivision, regular spacing of joints and chemical bond between the plates. This area is several years older than 1-75, but other than a few cracks, it appears to be in reasonably good shape.

3. Pavement Cracking

It is reported that cracking began immediately upon completion of the pavement. There are essentially three, types of cracking, namely: longitudinal, diagonal (at corners) and transverse. Longitudinal cracking is infrequent; isolated cases have been identified as those resulting from construction material related problems of the subgrade and as such, it will not be discussed in depth in this report.

Of those observed, almost without exception, the transverse cracks are in the long, 22.0 and 23.0ft sections, and they are located close to the center of the segment. They are either normal to the longitudinal joints or have a slight skew. The majority of diagonal cracking is associated with the acute corner area of the segments. These are obvious, repetitive patterns of cracking, which lead this author to believe that the distress of this pavement is related to the lengths of the sections and the, random, skew joints in the transverse direction.

Rehabilitation of the pavement is underway. It is done by partly removing the damaged sections, installing dowels and recasting the slab. During the night, previous to this author's visit to the site, the area received a heavy rainfall. Up to six inches of water collected where the slabs had been removed, turning the area into a series of artificial duck-ponds. The econocrete appeared to be in excellent condition; it is also completely impervious, thus not complying with the vital requirement of a well-drained subgrade. Extensive pumping under vehicular traffic has also been reported.

On the other hand, as it will be shown later, that vehicular traffic alone, even in the presence of free water, cannot possibly cause pumping. The premature signs of distress seem to indicate that temperature must have played a significant role in the I-75 problem. The distribution of temperature and its effect on stresses is not easy to understand, therefore a rigorous discussion of both questions will be given separately in the following chapters.

4. Distribution of Temperature

It is assumed for the computations that the area of pavement under consideration is exposed to uniform climatic conditions and no heat transfer is taking place in the two lateral directions. With this assumption, the three-dimensional "heat equation" is reduced to one dimension, which is depth.

$$\frac{\partial^2 T}{\partial z^2} = \alpha \frac{\partial T}{\partial t} \qquad (1)$$

where: T = temperature
z = depth
t = time
α = constant.

The meaning of this partial differential equation is that if there exists a continuous function T(z, t) that is twice differentiable with respect to "z" and once with respect to "t", the heat equation can be satisfied and T(z, t) is the distribution function of temperature. Finding such functions is not difficult, however, the problem is related to boundary conditions.

For any analysis, either closed format or based on relaxation techniques, a time domain has to be selected and either the distribution of temperature or its first derivative with respect to time be provided at both ends of the time domain. At the top of the pavement, variation in environmental temperature as a function of time has to be described in addition to some information as to what is happening to temperature deep in the subbase. These data can only be obtained by extensive monitoring of temperature on a long term.

Constant "ℓ" is the ratio of conductivity and specific heat of the concrete. A combination of high conductivity and low specific heat causes a rapid dissipation of heat which uniform temperature attains distribution through the physical domain. The combination of low conductivity and high specific heat, which is concrete, the dissipation is slow, leading to uneven temperature distribution, hence high stresses. Again, these values need be established for Florida concrete.

There is no known closed format function T(z, t), which would satisfy all possible initial values and boundary conditions. The best mathematicians have investigated the subject during the last three centuries and it is a favorite topic of textbooks dealing with applied mathematics. The avid reader is encouraged to get familiar with subject matter, even if and when

appropriate temperature database is available, a method of relaxation will be used for the analysis. This will be reported on in Part II.

5. Effect of Temperature Distribution

There are an infinite number of possible unique temperature distributions through the thickness of the concrete slab, some may be more critical than others. Instead of computation, a specific distribution will be selected, which is not contradictory to the limited data available (by others), and the I-75 pavement structure will be analyzed for that.

Let's assume that the distribution is in "steady state", i.e. independent of time. It is also continuous, but irregular, and for further manipulation it will be approximated by a polynomial through Taylor expansion or regression analysis:

$$T(z) \simeq \sum_{0}^{6} T_n \frac{z^n}{t^n} \tag{2}$$

where t: thickness of the slab.

In the following, equations will be developed to analyse the nature of the terms of the polynomial as functions of the power "n". Deformation of a unit length of slab is given in terms of $\varepsilon_z = \alpha\, T(z)$, where "$\alpha$" is the coefficient of thermal expansion. Figure 1 illustrates the geometry of the phenomenon. The deformations may be subdivided into three components, namely:

axial: $$\varepsilon_o = \frac{\alpha T_n}{n+1} \tag{3}$$

rotational: $$\varphi = \frac{6n}{(n+1)(n+2)} \cdot \frac{\alpha T_n}{t} \tag{4}$$

warping: $$\varepsilon_w = \alpha T_n \left[\frac{2(1-n)}{(n+1)(n+2)} + \frac{6n}{(n+1)(n+2)} \cdot \frac{z}{t} - \frac{z^n}{t^n} \right] \tag{5}$$

The axial component relates to the lateral expansion and contraction of the slab. This is not believed to be responsible for the I-75 problem, so it will not be further discussed. The rotational component is the most significant, for it causes the originally flat and straight segment to curl into a spherical shape, whose radius is:

$$r = \frac{1}{\varphi} = \frac{(n+1)(n+2)}{6n} \cdot \frac{t}{\alpha T_n} \tag{6}$$

In a simply supported bridge structure, this curling effect is harmless in terms of developing stress, since the structure is free to heave and sink between its supports. In a rigid pavement, the self weight of the slab and the

axle loads tend to uncurl the segment through flexure. It will be shown that both the flexural stresses and the magnitude of separation between the slab and the subgrade increase with the length *of* the segment and the stiffness "k" *of* the subgrade.

It is *a* fundamental structural engineering principle that in the elastic range the cross section of a prismatic component remains straight. Any nonlinear (n>l) temperature distribution would cause a warping of the cross section. Stresses f = E to be called primary temperature stresses for the rest of this report, are de-warping the cross section causing it to remain straight. Axial and rotational deformations are not being effected by primary stresses. In Table I, pertinent deformation values are provided as a function of power "n".

It can be seen that the axial component is decreasing as "n" increases, as expected. The rotational component is fairly constant for the range considered, and the tensile warping stresses both at op and bottom of the slab increase with "n". In order to illustrate the computations, an example is given below. The selected values are believed to reflect extreme conditions prevailing at the I-75 roadway.

e.q. $n = 4$
$T_n = 30°F$
$t^n = 9$ inches
$E = 3{,}500{,}000$ psi
$\alpha = 0.000006$ in/in
$\alpha T_n = 6 \times 30 = 180\mu$

Figure 2 illustrates the breakdown of temperature deformations. Stresses are given in psi, deformations in microstrains ($\mu \times 10^{-6}$ in/in).

Top and bottom tensile stresses due to warping are 252 and 126 psi, respectively. The maximum compressive stress is 100 psi. For a positive temperature input, tensile and compressive stresses are reversed, indicating that for an identical distribution, cooling causes higher tensile stresses.

The dramatic effect of primary stresses can be observed in factories, which are producing architectural and/or commercial (like patio stones) concrete products. Often an autoclave, with high steam pressure and temperature, is employed to obtain quality economically. At the end of the process, the product is cooled down to a temperature just below boiling point. It has been observed that if, upon removal from the autoclave, the product is exposed to a cool draft, and it will destroy itself in an explosive manner.

Corresponding radius of curvature "r" is 62,500 inches, or approximately one mile. One way of visualizing the curled shape of a segment is to take a thin-walled sphere of about two miles of diameter and cut out a part along the contour lines of a segment. Figure 3 illustrates this by picturing a short and a long segment adjacent to each other. The deformations (given in 10 inches) do not include the effect of self-weight of the slab, so the actual prototype values are smaller than those shown. Nevertheless, a mismatch between segmental deformations is obvious; the difference is maximum at the acute corner of the larger segment. As the segments are tied together by dowels,

they are in effect fighting each other, shear forces are transmitted through the transverse joint, causing positive moments in the short segment and negative moments in the long one:

Vertical deformations are calculated from the following formula:

$$d = \frac{g^2}{2r} \qquad (7)$$

Where "g" is the radial distance between the centroid of the segment and the point under consideration.

6. Interaction Between Slab and Subgrade

The behavior of plates under loads acting perpendicular to their planes had concerned the early researchers at the time of the industrial revolution and it was the French mathematician Lagrange, who in 1811 succeeded in describing flexural plate responses by a fourth order differential equation:

$$\frac{\partial^4 z}{\partial x^4} + \frac{2\partial^4 z}{\partial x^2 \cdot \partial y^2} + \frac{\partial^4 z}{\partial y^2} = \frac{w}{R} \qquad (8)$$

Where: z: displacement perpendicular to the plate
x and y: lateral coordinates
w: distributed vertical load
R: $Et^3/12(1-\nu^2)$
E: modulus of elasticity
t: thickness of plate
ν: Poisson's ratio

Solutions of Equation 8 for uniformly distributed loads had been obtained with relative ease, however, Fourier and other representations of concentrated (wheel) loads consistently failed due to mathematical instability (divergence). In 1925, the Hungarian mathematician Nadai (University of Berlin), by a deductive process involving functions of a complex variable, derived a solution in finite (closed) format. In 1930, Westergaard brought Nadai's work to America and it became, and still is, the basis for the design of both rigid pavements and bridge deck slabs.

This all is, however, only of historic concern. For the combination of dead weight, wheel loads, temperature and various boundary conditions - closed format solutions are of little practical use and one has to resort to relaxation methods. At present, an effort is underway to develop a generalized relaxation method based on the principles of finite differences by which the plate (segment) can be analyzed for various combinations of effects. The analysis may include the solution of several thousand simultaneous equations, for which either the FDOT mainframe computer has to be upgraded or outside computer facilities be utilized.

Due to limitations in available time and computing facilities, and for the purpose of this report, a one-dimensional version of the Lagrange equation will be used. Consideration for subgrade reaction and the effect of temperature (curling due to sectional rotation) is introduced as follows:

$$R \frac{\partial^4 z}{\partial x^4} + k(z - z_T) = w + q \tag{9}$$

Where: R = E.J - sectional rigidity
J = inertia
k = modulus of subgrade
z_T = unrestricted deformation due to temperature
w^T = weight of slab
q = wheel load (distributed over a patch)

Equation 9 can be rearranged to separate from what will be known as normalized stiffness matrix (LHS) from load column matrix (RHS):

$$\frac{\partial^4 z}{\partial x^4} + \frac{k}{R} z = \frac{w + q}{R} + \frac{k}{R} z_T \tag{9a}$$

A particular solution (not including temperature effects) had been provided by the German railway engineer Zimmerman to analyze the interaction between the rail-tie superstructure and the ballast at the end of last century and it is still being used. The complete solution for Equation 9a is if:

$$p = k z_T = [3x^2 - a^2] \frac{k}{6r} \tag{9b}$$

$$\beta = \sqrt[4]{\frac{k}{4R}} \tag{9c}$$

where "a" is the half length of the segment,

$$z = e^{\beta x}[C_1 \cos \beta x + C_2 \sin \beta x] + e^{-\beta x}[C_3 \cos \beta x + C_4 \sin \beta x] + \frac{3x^2 - a^2}{6r} + \frac{w + q}{k} \tag{10}$$

Zimmerman had little difficulty in evaluating the equation as for a rail of infinite length, coefficients C_1 and C_2 disappear and the rest is available in textbooks on advanced strength of materials. Our case is more complicated. All the four coefficients exist and they can only be defined by introducing boundary conditions.

The dimension of "β" is in^{-1} and its inverse $b = \beta^{-1}$ is referred to as the "characteristic length". It will be shown later that the ratio βa = a/b is a major parameter for the analysis and that "b" can be used for first estimates in design.

In order to study the temperature effect separately, the last (load) term is eliminated from Equation 10. Boundary conditions are that moment: $M=-R\ddot{z}$ and shear: $V=-R\dddot{z}$ are zero at both ends of the segment. The coefficients are:

$$C_1 = \frac{1}{4\beta^2 r} \cdot \frac{T-t}{T(1-t^2)-t(1+T^2)} \cdot \frac{1}{\cos\beta a \cosh\beta a} = C_3 \qquad (11)$$

$$C_2 = \frac{1}{4\beta^2 r} \cdot \frac{T+t}{T(1-t^2)-t(1+T^2)} \cdot \frac{1}{\cos\beta a \cosh\beta a} = -C_4 \qquad (12)$$

Where $T = \tanh\beta a$ (hyperbolic tangent)
$t = \tan\beta a$ (trigonometric tangent)

Ground pressure between the segment and subgrade is the product of the segment rigidity and the fourth derivative of the deflection curve:

$$p = R\ddot{z}'' = -4\beta^4 R\left[C_1 \cos\beta x \cosh\beta x + C_2 \sin\beta x \sinh\beta x\right] \qquad (13)$$

Equation 13 is then evaluated for the I-75 combination of parameters:

length of slab: l = 23'-0 and a = 138 inches
subgrade stiffness: k = 200 x 144 = 28,800 lb/in^2
inertia: I = 1/12 x 144 x 9^3 = 8748 in^4
modulus of elasticity: E = 3,500,000 psi
Using equation (9c) β^{-1} = b = 45.411 in. and βa = a/b = 3.0389112
For temperature radius r = 62,500 inches:
C_1 = +.866018 x 10^{-3} and C_2 = +.703542 x 10^{-3}

Distribution of ground pressure is illustrated in Figure 4 with respect to the dotted line. It can be seen that in the central part, the pressure is negative (tension), i.e. the slab is trying to separate from the subgrade. After normalizing the curve with the dead weight of the slab: w = 112.5 lb/in - compression is observed along the full length of the segment. The maximum combined pressure of 588.51 lb/in occurs at the ends. Corresponding pressure is 588.51 ÷ 144 = 4.087 psi and z = 4.087÷ 200 = .0204 in. is the deformation.

The reader may note that the diagram in Figure 4 is valid only for positive temperature (warming) input. For negative (cooling) input, the slab dead weight is deductive, causing separation of the ends of the segment which in turn makes the above computations invalid. This subject will be discussed later.

Moment along the length of the segment is obtained as a product of the segment rigidity and the second derivative of the deflection curve (dead weight does not cause moment by itself).

$$M = -R\ddot{z}' = -4R\beta^2\left[-C_1 \sin\beta x \sinh\beta x + C_2 \cos\beta x \cosh\beta x\right] - \frac{R}{r} \qquad (14)$$

Moments are calculated for the same set of parameters as before and illustrated in Figure 5. Maximum value of + 533,860 lb/in occurs at the centerline of the segment and the curve tapers to zero at the ends. The dotted line indicating M_0 = + 491,904 lb/in corresponds to a joint less, continuous pavement and is defined as M_0 = + R/ r.

The sectional modulus of the 12.0 ft. wide pavement is S = 144 x $9^2/6$ = 1,944 in^3. Therefore the maximum secondary temperature stress due to restricted curling is f 533,860 ÷ 1944 = 275 psi compression on the top and tension on the bottom.

Further manipulation of Equation 14 yields:

$$f^{T}_{max} = \pm \frac{C_n E_c T_n}{2(n+1)(n+2)} \left[1 - \frac{2(t+T)\cos\beta a \cdot \cosh\beta a}{\sin 2\beta a + \sinh 2\beta a} \right] \qquad (15)$$

It can be seen that stresses are independent of the thickness of the slab. In the next chapter, a parametric study will be carried out to establish their relationship to the stiffness of subgrade, rigidity of slab and length of segment.

7. Temperature Stress as Function of "k", "R" and "a"

For this study, only the bracketed term of Equation 15 need be evaluated. The following parametric spectra were considered:

Elasticity: E = 2,500,000 to 4,000,000 psi
Thickness: t = 6.0 to 12.0 inches
Subgrade: k = 40 to 500 pci (for 144 in wide lane: 5,760 to 72,000 lb/in/in)
Length: l = 10.0 to 23.0 ft. (a = 60 to 138 inches)

These values yield: b_{max} = 87.117 inches for (βa) min = 0.6887 and b_{min} = 24,495 inches for (βa) max = 5.6338

The actual calculations were carried out in $\Delta(\beta a)$ = 0.2000 intervals between 0.6 and 5.6. Figure 6 illustrates the outcome of the investigation. The curve rises from zero to a maximum value of 1.08623 at $\beta a = \pi$ = 3.1416 and then it approaches 1.0 asymptotically for larger values of βa. For previous calculations regarding I-75, the value of "b" was estimated to be 45.411 inches. Then a values for various segment lengths are:

l = 16'-0	a = 96 inches	βa = a/b = 2.114
17'-0	102 inches	2.246
22'-0	132 inches	2.907
23'-0	138 inches	3.309

It has been observed that the majority of the transverse cracks have occurred in longer segments. The value corresponding to the 23.0 ft. length approaches the absolute maximum on the curve. The conclusion, which may be drawn is that moments due to temperature are rapidly increasing with the length of the

segment. An improved design can be achieved if the βa variable is kept below 2.0. This can be attained by a combination of reduced segmental length, reduced subgrade stiffness and increased slab rigidity.

8. Stresses due to Axle Loads

Deflections and moments were computed for axle weights both by relaxation and in closed format, although the latter was restricted to central load position only due to mathematical complexity. Without formal proof, the deflection diagram of a 23.0 ft. long segment is illustrated in Figure 7. The distribution is quite wide spread, engaging the internal 198 inches of the 276 inches long segment in compression. It may be noted that the maximum pressure under a 27,600 lb. axle is only 2.141 psi.

Figure 7 also indicates the characteristic length "b" on either side of load "P". It would appear that a rather good first estimate of peak pressure can be obtained by distributing the load on a length of 2b; hence $p_{max} = P \div 2 \times 45.411 = Px11.0105 \times 10^{-3}$; the error is only 1.4 percent. It is obvious that this approximation is invalid when the axle is closer to the end of the segment than "b".

As part of this particular analysis, a closed format equation has been obtained for positive moment under a centrally located concentrated load.

$$M_o = \frac{Pb}{4}\left[1 - \frac{e^{-\beta a}}{\cos\beta a} \cdot \frac{t(1-t)+T(1+t)}{t(1-T^2)+T(1+t^2)}\right] \qquad (16)$$

Equation 16 has been evaluated for various combinations of segmental half-length "a" and characteristic length "b"; the results are plotted in Figure 8. It can be seen that the moment values are narrowly banded between Pb/4.0 and Pb/3.7, again providing for a reasonably precise first estimate.

For load positions, other than central, a relaxation method based on generalized finite differences has been utilized. Here the length of the segment is subdivided into "n" equal spaces. Parametric studies, not reported herein, indicated that n = 120, i.e. a subdivision length h = 2.30 inches, would produce as precise results as can be expected. Mathematically, this subdivision provides for 121 simultaneous equations by which differential Equation 9a is satisfied on a pointwise basis. For this process for fourth derivative term is approximated by:

$$\frac{\partial^4 z}{\partial x^4} \simeq \frac{+z_{i-2} - 4z_{i-1} + 6z_i - 4z_{i+1} + z_{i+2}}{h^4} \qquad (17)$$

where "i" is a running point from 1 to 121. For i = 1, 2, 120 and 121, some of the nodes become phantom; they are replaced by appropriate boundary conditions. There is a beautiful mathematical symmetry in the fact that the number of phantom nodes is always equal to the number of boundary conditions available.

The axial load "P" is assumed to be distributed on the top of the pavement in a trapezoidal manner as demonstrated in Figure 9.. The bottom of the trapezoid is "5h" wide, the height is in our case 3,000 lb/in. What the computer sees is a sequence of five small concentrated forces applied at the nodes. Admittedly, there is an arbitrary element in deciding upon representing an axle load as being transmitted to the pavement. The nature of this representation effects the moment under the load only.

The output of the analysis is a deflection (z.) diagram given in a discrete form at the nodes. Moment at any point (node) "j" can be computed from:

$$M_j = \frac{R}{12h^2}\left[z_{j-2} - 16z_{j-1} + 30z_j - 16z_{j+1} + z_{j+2}\right] \qquad (18)$$

The 27,600 1b. axle weight was moved along the length of the segment between nodes 3 and 119. For each load position deflections and moments were computed. Figure 10 displays the moment diagram due to a central load location in addition to moments occurring under the moving load. The latter can be taken also as maximum positive moment diagram for a single axle.

Closed format Equation 16 yields M = + 11.3125 P; for our case of concentrated load P = 27,600 lb. the central moment is + 312,225 lb./in. The value obtained through relaxation is 283,000 lb./in; the difference between the two is due to the patch load distribution applied in the latter. It appears that the positive moment is slightly increases towards the quarter points and then rapidly approaches zero towards the ends of the segment. Flexural stress at center therefore is 283,000/1944 = 146 psi:

The strength of a 22,000 lb. rated capacity axle at ultimate limit states is about 55,000 lb. For this study, an axle load of 1.5 x 27,600 = 41,400 lb/in. assumed. This assumption requires verification in light of the fact that others regarding the permissible axle weights of 22,000 lb have observed dynamic amplification of 1.75 to 2.00.

Figure 11 exhibits the maximum positive moment diagram due to a 41,400 lb. single axle and to a 30°F temperature differential curling (see Figures 5 and 11). The maximum value of 958,360 lb/in. occurs at the center and the corresponding, tensile stress is 493 psi at the bottom of the slab. This, together with the primary tensile stress due to temperature warping of 126 psi, gives a maximum of 619 psi, which exceeds the tensile strength of the concrete. The maximum moment diagram is rather flat at center, indicating that the probability of failure along the central third of the segment is fairly uniform.

9. Magnitude of Temperature Loads

Temperature effects have never been properly considered in the design of concrete pavements and the reader may feel surprised about their magnitude relative to those of commercial vehicles. Equation 9a treats the product kz_T as a pseudo load and in the following it will be closely examined for

distribution and size. The distribution of this pseudo loading due to restricted temperature curling is given by Equation 9b, expressing that the pressure is proportional to the subgrade coefficient "k". The radius of curvature of the segment is "r" and the loading is in equilibrium (no outside forces).

Integrating the pressure between $x=-a/\sqrt{3}$ and $x=+a/\sqrt{3}$, force "P" can be determined:

$$P=\pm\frac{2ka^3}{9r\sqrt{3}} \tag{19}$$

It is interesting to note that "P" is proportional to "k" and "a^3", indicating that in order to minimize stresses due to curling, both "k" and "a" values are to be kept low.

10. Shear Transfer at Joints

Structural characteristics and strength of shear transfer hardware are very important in the design of rigid pavements. In this chapter, the combination of slab and hardware characteristics will be examined with respect to shear transfer between the segments under moving axle loads. After some rather complex manipulation, a closed format solution of deflection for a shear force "V", applied at a joint x=-a, has been obtained:

$$Z=\frac{-V}{4\beta^3 R\cos\beta a\cosh\beta a}\cdot\frac{1}{AB}\left\{\begin{array}{l}\cos\beta x\,[A\cosh\beta x+TB\sinh\beta x]+\\ -\sin\beta x\,[tTA\sinh\beta x+tB\cosh\beta x]\end{array}\right\} \tag{20}$$

where: $A = -T(1+t^2) + t(1-T^2)$
$B = +T(1+t^2) + t(1-T^2)$
$T = \tanh\beta a$
$t = \tan\beta a$

Equation 20 has been evaluated for the assumed I-75 parameters and the deflection diagram is depicted in Figure 13. The curve indicates a hyperbolically dampened trigonometric function as expected, with most of the activity taking place on the left-hand half of the segment. Actual deflections can be obtained by multiplying the ordinates with a given "V" force. The end shear spring constant of the segment is the invert of the ordinate at the end:

$$S = (1.529266 \times 10^{-6})^{-1} = 653{,}908 \text{ lb/in.}$$

The spring constant is also available in closed format:

$$S=kb\,\frac{-AB}{A(1+t^2T^2)-B(t^2+T^2)} \tag{21}$$

For practical combinations of parameters, "S" can be approximated by:

$$S = 0.5kb \tag{21a}$$

which for our case yields .5x28,800x45.411 = 653,918 lb.

Based on the principle of Mueller-Breslau, the deflection diagram due to a pair of 0.5S forces will become a shear transfer influence line, which can be further normalized for the patch distribution of the axle load as illustrated in Figure 14.

It can be seen that due to the finite width of the patch, maximum shear force occurs when the axle is about 5.75 inches away from the joint. The shear is 37.4 percent of the axle weight. It is also evident that the next axle (second of a tandem), being 51 in. away from the leading one, causes only negligible effect. It would appear that as long as the characteristic length "b" does not exceed the wheelbase considerably, the second axle can safely be ignored for the computations.

The influence line in Figure 14 is based on the assumption that the shear transfer hardware (dowels) have no play (slack) in them and that they are infinitely stiff with respect to shear. Neither of these assumptions is strictly correct, and their effect will be examined in the following.

As demonstrated in Figure 15, the total apparent shear deformation "Δ" has two components: one is related to the lack of fit (slack) of the dowel in the concrete hole, the other to the elastic deformation of the dowel itself. Both halves of the dowel are assumed to be in contact with the concrete at two points only; these points are at a distance "c" from the end of the dowel and from the end of the concrete segment.

From the point of view of rigorous analysis, this model is admittedly weak. Yet due to the fact that distance "c" must be larger than zero, but smaller than about one-twelfth of the dowel length, a reasonable good estimate of the displacements and forces that play a role, can be obtained:

Equation 22 provides for shear deformation:

$$\Delta = 2s\frac{l-c}{l-2c} + \frac{2Vc^2(l-c)}{3EJ} \tag{22}$$

Where: l: half length of the dowel bar
s: play between the dowel and the hole (slack)
E: modulus of elasticity of the dowels
I: inertia of the dowels

For the first leg of this examination, slack "s" is assumed to be zero. Using 12 dowels of 1.0 in. diameter, 18 inches long with a modulus of elasticity of 29×10^6 psi:

$$3EI/2 = 25{,}623 \times 10^3 \text{ lb.in}^2$$

As before, the coefficient of shear transfer is defined:

$$K_D = \frac{V}{\Delta} = \frac{3EJ}{2c^2(\ell - c)} \qquad (22a)$$

if c = 0.0 in	K_D = infinity
= 0.5	= 12,057,882 lb/in
= 1.0	= 3,202,875 lb/in
= 1.5	= 1,518,400 lb/in

It is therefore obvious that no matter what the actual "c" value may be, the effect of elastic deformation of the dowel system having a perfect fit, regarding the quality of shear transfer, is minimal.

For the second leg, only the slack related term in Equation 22 will be considered. If "s" is 10 mills and "c" is 1.50 inches, total deformation neglecting the contribution by the dowels is .025 inches. This, in combination with the previously calculated shear spring stiffness of the concrete slab proper, means that up to V = .025 x 653,918 = 16,348 lb, no shear transfer can develop between the segments. On the other hand, the same dowels permits the segment fighting each other when differential curling occurs due to temperature. As shown in Figure 3, at the acute corners this difference is 221-98=123 mills, far exceeding the slack.

It can be concluded therefore that the presence of dowels with any appreciable slack with them could be detrimental to concrete pavements by way of denying shear transfer capability under vehicular loading but transmitting temperature induced forces. It can be stipulated that the application of dowel bars as shear transfer devices may be counter-productive under certain parametric combinations.

11. Separation due to Negative (cooling) Temperature Input

In Figure 4, the interaction between slab dead weight and downward curling due to a positive (warming) temperature loading has been illustrated. It was found that the dead weight is sufficient to control the tendency of the slab against uplift, resulting in compressive stresses between the segment and the subgrade on its full length. The effect of negative temperature loading is exhibited in Figure 16.

It can be observed that at both ends of the segment, for a length of approximately 23.5 inches, the net interface stress is tensile. The segment, however, has no bond to the subgrade, consequently, actual tension cannot develop and separation must take place.

The mathematical simulation of separation involves an iterative process, in which the shapes of the deflection curve is estimated and along the lengths were the deflection is negative, "k" value is taken as zero. With this a round of calculations is carried out and repeated until the calculated deflection pattern matches the assumed one. To do this in closed format is not possible, but it can be done with relative ease by the computer.

Figure 17 reveals the actual deflection shape of the segment under the combination of self-weight and negative temperature curling. It can be seen that the shape changed considerably and the length of separation is 53.7 inches at both ends. The upward net movement of the end points is -49.5 mills; similar measurements have been reported by our Bureau of Materials and Caltran (California DOT).

Figures 18a-to-18f illustrate the effect of a 41,400 lb axle load, in addition to self-weight and temperature, moving from center towards the end of the segment. As the load moves, the separation at the front end becomes smaller and it entirely disappears when the load is about 48 inches from the end. At the same time, the tail end goes through some contortions but stays in the air during the whole action.

If the negative temperature input is the result of a sudden rainfall of high intensity, it is likely that the shaded area in Figure 18a is full of water. The approximate volume of the water is: V = 0.5 x .0526 x 55.6 x 144 = 210 cubic inches, or close to a gallon. The length of travel of the axle load before the gap disappears is 138-48 = 90 inches. If the vehicle travels at 60 miles/hour (1008 in/sec), it takes t = 90/1008 = .0893 seconds to do so. The subgrade being impervious, the water can only escape through the joints and cracks. The average area of the two side openings during this action is A = 0.5 x .0526 x 55.6 = 1.463 in^2. The average velocity of water, while escaping, is 210/1.463 = 143.6 in/sec. If the water were forced to escape through the side joint, it would result in a miniature geyser of 26.7 inches high. This action has been often observed on the pavement.

It can therefore be concluded that curling due to negative temperature input permits the development of a perfect pump under moving axle loads. The velocity of the escaping water is also high enough to mobilize the fine particles in the subgrade and thus causing changes in the subgrade with detrimental consequences. One beneficial effect of the econocrete is that it does not contain movable particles.

12. Critical Length of Segment

If an axle load is applied to one end of a segment, the other end tends to lift up. Such action is conducive to rocking and pumping, and should therefore be avoided. If x = +a is substituted in Equation 20, this particular problem can be studied in closed format. Deflection at the RHS end, for a load applied at the LHS end, is as follows:

$$z_{END} = \frac{-V}{4\beta^3 R} \cdot \frac{(1-T^2)(1+t^2)[t(1+T^2) - T(1-t^2)]}{A \cdot B} \qquad (20a)$$

This can be rewritten in a simpler form:

$$z_{END} = -\frac{V}{kb}\gamma \qquad (20b)$$

where $\gamma = (1-T^2)(1+t^2)[t(1+T^2) - T(1-t^2)] \div AB$

The parameter "γ" is evaluated for "βa" values larger that 0.6 and the outcome is manifested in Figure 19. The curve, as expected, starts out with a large negative value at $\beta a = 0.6$, then crosses the zero line at about $\beta a = 1.98$ and disappears around $\beta a = 2.4$. Separation occurs when the pressure between the segment and the subgrade becomes zero:

$$p = kz_{END} - w = 0$$

The critical "γ" value can be defined as:

$$\gamma_{cr} = \frac{-wb}{V}$$

In our case: w = 112.5 lb/in
b = 45.411 inches
V = 41,400 lb so

$$\gamma = -112.5 \times 45.411 \div 41{,}400 = -.1234$$

This corresponds to $\beta a = 1.648$ as displayed in Figure 19. This leads to
$a_{cr} = 1.648 \times 45.411 = 74.84$ inches and
$l_{cr} = 2 \times 74.84 = 149.67$ inches = 12.47 ft.

It has been concluded in Chapter 7, that in order to reduce temperature stresses, the value of "βa" should be kept below 2.0. The above calculations seem to indicate on the other hand that "βa" should not be less than 1.65. Thus a rather narrow band of a design spectrum has been determined, outside which the performance of the pavement is not likely to be satisfactory. As established earlier, the I-75 "βa" value is 3.03. For the lack of appropriate testing procedures, it is not certain as to what the actual I-75 "k" value might be. For this investigaton, k=200 pci has been assumed. If that value is 500 pci for the econocrete subgrade, as reported, the actural "βa" value may be as high as 3.82, being clearly outside the preferred range of design.

Determining the critical minimum length allows to draw further conclusions. When a segment breaks due to overstress, it becomes two segments. The critical length definition applies to the reduced lengths. If a 23.0 ft. long segment breaks at center, it produces two new segments of 11.5 ft. long, both being shorter than the critical length. The present method of rehabilitation is to create a new transverse joint at center. This solution may not prove to be satisfactory on the long term.

13. Maximum Longitudinal Negative Moments

Maximum negative moments occur in the slab when the axle load is located in the end zone. If there is one axle at each end, the flexural effect is cumulative. Figure 20 displays moment diagrams due to two moving axles, located symmetrically with the centerline of the segment. As before, the analysis includes the effect of self-weight, temperature, axle loads and separation of subgrade, when it occurs. The axle loads are 41,400 lb. each and are distributed as depicted in Figure 9.

The maximum moment is - 728,000 lb.in., causing a top tensile stress of -374 psi. As shown in Figure 2, the top primary temperature stress is 252 psi. The sum of these is -626 psi, which again exceeds the tensile strength of the concrete.

The conclusion is that the slab may break for either positive or negative temperature input and the crack will always be located in the central third of the segment.

14. Corner and Longitudinal Cracks

On I-75 many segments have also suffered corner breaks. The cracks invariably occur at the acute angle of the segment and they are directed diagonally. The one-dimensional simulation of the slab does not permit a rigorous analysis of diagonal stresses. A two dimensional analysis may require the solution as many as 7,500 simultaneous equations, a task which exceeds the capacity of FDOT's mainframe computer. This work will be done at a later date (Part II).

Figure 21 illustrates the moment diagram for a unit load applied at the LHS end of the segment. This diagram will be used to approximate the action-taking place in the corner zone.

It can be seen that the maximum moment occurs at a distance approximately 36 inches from the end. At that point, counting from the tip of the acute corner, the shortest diagonal of the segment is about 61 inches. Sectional modulus for this width is 824 in. If the tensile strength of the concrete is 600 psi, of which 252-psi primary stress is deducted, the force required to break the corner can be estimated as:

$$M = 6.79 V_{CR} = 824 (600 - 252)$$

$$V_{CR} = 824 \times 348 \div 6.79 = 42,232 \text{ lb.}$$

If the half axles load: 0.5 x 41,400 = 20,700 lb subtracted from this, there remains 21,532 lb/in. be accounted for. But if the differential deformation of (.221 - .098) = .123 inches, shown in Figure 3, multiplied by the half stiffness of the slab calculated in Chapter 10: .123 x 0.5 x 653,918 = 40,217 lb, it is obvious that the corner may break down under the combined effects of axle load and differential temperature movement between adjacent segments.

There are also some longitudinal cracks. Most of them have been identified as the result of expansive aggregate in the econocrete subgrade. But if the tie bars along the longitudinal joints cause transverse flexural continuity, a length of 24.0 develops which is vulnerable to restricted temperature curling stresses as discussed throughout this report.

15. Limit States Design

At present, the design of rigid pavements is carried out by the application of a single equation by which the number of 18 Kip equivalent axle loads is predicted. The outcome is the function of the following:

thickness of slab
serviceability indices
modulus of rupture
shear transfer
drainage
modulus of elasticity
modulus of subgrade.

In the previous chapters of this report, it had been demonstrated how many different aspects need be investigated and how complex the analysis may become even with a one-dimensional simulation of the pavement. The credibility of this equation is therefore rather low.

Furthermore the equation is based on working stress and fatigue considerations, and it is believed to have been borrowed from flexible pavement design. The significance of temperature effects is demonstrated by the presence of cracks in pavements prior to being opened to traffic. The general performance of rigid pavements, and in particular the I-75 problem seem to indicate that these considerations are invalid and the proper design method should be derived by using the principles of limit states.

For the design of concrete pavements, only ultimate limit states (cracking) need be considered. For this, a desired safety index "β" can be set, which is the function of safety (number of failures expected) and economy (cost of replacement of failed components). For bridge structures, the primary aspect is safety and the "β" value is set as high as 3.5. This represents a failure rate of two parts per million per year, which translates to one failure in 50 years in a bridge population of ten thousands. For pavement structures, the significance of safety is much lower, consequently a lower "β" can be envisioned. The proper value can only be arrived at through studies of economy. The equation for "β" is:

$$\beta = \frac{\ell_n R - \ell_n S}{\left[w_R^2 + w_S^2 \right]^{1/2}} \qquad (23)$$

Where: R: mean resistance or strength
S: mean load or stress
w_R: coefficient of variation of resistance
w_S: coefficient of variation of load

All the four variables are statistical in nature and the database required for their evaluation is not available. The numerator is the ratio between the means of resistance and loading, and is usually referred to as "factor of safety". Ws is related to the statistical spread in self-weight, temperature and axle weight variations. Wr includes the spread for subgrade resistance, reliability of shear transfer hardware, thickness and the tensile strength of concrete.

In order to determine the strength of the I-75 concrete, 66 cores were taken and tested for modulus of elasticity and compressive strength. The latter was analyzed statistically and it was found that the mean (average) strength is 5,040 psi, standard deviation 714 psi and the coefficient of variation 14.16 percent. The tensile strength associated with the mean is 7.5 x $\sqrt{}$ 5,040 = 532 psi, is considerably lower than the calculated maximum stress due to the combination of self weight, temperature and axle load.

The proposed limit states process provides for a proven framework of reference by which long-lasting pavement structures could be designed in future. Data required for this process, however, are completely different from those currently being collected.

16. Field Testing Procedures

At present, there are three structurally oriented field-testing procedures: modulus of subgrade, deflection of pavement and temperature. In the following, these will be reflected upon separately.

16.1 Modulus of Subgrade

Using modified AASHTO Standard T-222-78 “No repetitive Static Plate Load Test of Soils and Flexible Pavement Components” carries out determination of subgrade “k” values. The equipment used features, a 30 in. diameter disc by which the load is applied. This diameter reflects the rather small "characteristic radius" (length) associated with flexible pavements. The radius for concrete pavements is much larger, the attendant interface pressure is smaller, and it is believed that T-222-78 may not be applicable. It is recommended that the disc diameter should not be less than 60 inches and the process include repetitive testing in order to establish the increase in "k" value due to consolidation (shake-down).

16.2 Deflection of Pavement

Deflections due to static loading or falling weights are measured on a routine basis. The author is not familiar enough with this testing process to offer any comment. But the deflection of concrete pavements is very small (not likely to exceed 20 mills) and the calculations by which moments and interface pressures (first and second curvatures, respectively) are determined are extremely sensitive for the slightest error in measurements.

In the previous two chapters, two distinct sources of temperature effects have been identified and quantified: namely primary stress and stress (secondary) due to restricted curling. The primary stresses are completely locked in and can’t be measured by deflections of for that matter by strains. As far as secondary stresses are concerned, only the restricted deformation can be measured. Higher the level of restriction, lesser is the chance to obtain meaningful observations. Only force measurements are effective, but for that extensive laboratory facilities are required.

16.3 Temperature

At present, temperatures are taken (by thermocouples) at two points, namely at top and bottom of the slab. This is not satisfactory. If the temperature distribution polynomial is of the order of "n", the minimum number of observation points along the depth of the slab is "n + 1". Thus, for a fourth order curve, at least five thermocouples are requires, in addition to some to be located in the sub grade.

Extreme temperature conditions that are detrimental to the pavement do happen unexpectedly and infrequently; they also last only for a short period of time. In order to capture these events, short-term monitoring efforts are not likely to succeed. To collect field data at the time of sudden cooling or intensive rainfall could be an unpleasant enterprise. For this purpose, a fully automated data acquisition system, capable of continuous year-round observation, is required.

17. Conclusions

17.1 The calculations indicate that temperature should be considered in the design of rigid pavements.

17.2 The I-75 problem is the result of an unfortunate combination of design features, namely a too rigid subgrade, excessive length of segments, the random variation of lengths, the skewed transverse joints, and the effects of temperature.

17.3 In the event of sudden cooling, the long segments separate from the subgrade and, in the presence of free water, extensive pumping takes place. The effects of pumping on I-75 have not been identified.

17.4 An improved design method may be found in terms of limit states design, but for this a major testing program must be undertaken.

18. Recommendation

In no particular order of importance the following projects are recommended to clarify various aspects for the design of concrete pavements:

18.1 Thermal conductivity and specific heat of Florida concrete and subgrade.

18.2 Distribution of solar heat between the environment and pavement structure.

18.3 Heat transfer as function of temperature difference and the rate of temperature change.

18.4 Verification of primary and secondary temperature stresses predicted by analysis.

18.5 Effect of non-linear distribution of moisture content.

18.6 Tensile strength of concrete exposed to stresses of non-linear distribution.

18.7 Feasibility of increasing the tensile strength of the top layer of concrete by water curing and/or other methods of construction.

18.8 Establish subgrade "k" values using plates of large radius approximating the characteristic length.

18.9 Variation in "k" values due to repeated loading and/or moisture.

18.10 Effectiveness of dowels for small movements.

18.11 Develop hardware providing for improved joint control and elastic shear transfer.

18.12 Fatigue strength of shear transfer devices.

18.13 Verification of two dimensional stress distribution in rigid pavement due to vehicular loading predicted by analysis.

18.14 Effect of inertial forces and resonance on stresses and fatigue life.

18.15 Boundary conditions required to ensure permanent recompressions in the subgrade.

18.16 Optimum embankment geometry to eliminate transverse tension in pavement.

18.17 Optimum grading of subgrade to obtain stable construction under turbulent flow conditions.

TABLE I

n	$E_o/\alpha T_n$	$\varphi/\frac{\alpha T_n}{t}$	$\varepsilon_w/\alpha T_n$				
			z=o*	.25t	.50t	.75t	t
0	1.000	0	0	0	0	0	0
1	.500	1.000	0	0	0	0	0
2	.333	1.000	- .1667	+ .0208	+ .0833	+ .0208	- .1667
3	.250	.900	- .2000	+ .0094	+ .1250	+ .0531	- .3000
4	.200	.800	- .2000	- .0039	+ .1375	+ .0836	- .4000
5	.167	.714	- .1905	- .0129	+ .1354	+ .1079	- .4762
6	.143	.643	- .1785	- .0181	+ .1272	+ .1256	- .5357

*Note: z=0 is at the bottom of the slab.
$\varepsilon_w/\alpha T_n$ values are for a negative (cooling on top of slab) temperature distribution.

References

1. "Computation of Stresses in Bridge Slabs due to Wheel Loads" by H. M Westergaard, Public Works, March 1930

2. "Advanced Strength of Materials"' by Den Hartog, McGraw Hill, 1952

3. "Fourier Series and Boundary Value Problems" by Ruel V. Churchill, McGraw Hill, 1963

4. "Relaxation Methods" by F. S. Shaw, Dover 1953

5. "Load Factor Design" by K. Ravindra and T. Galambos ASCE, 1973

6. "Differential Equations" by R. P. Agnew, McGraw Hill, 1960

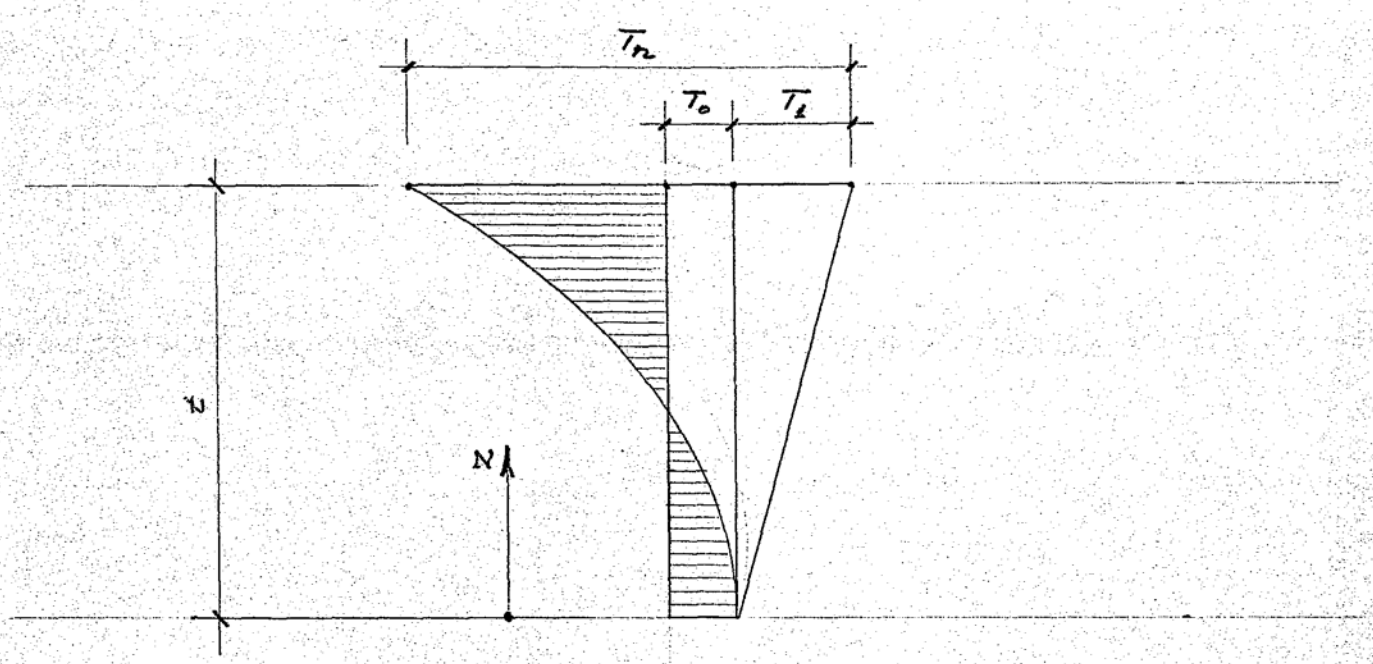

TEMPERATURE DISTRIBUTION

Figure 1

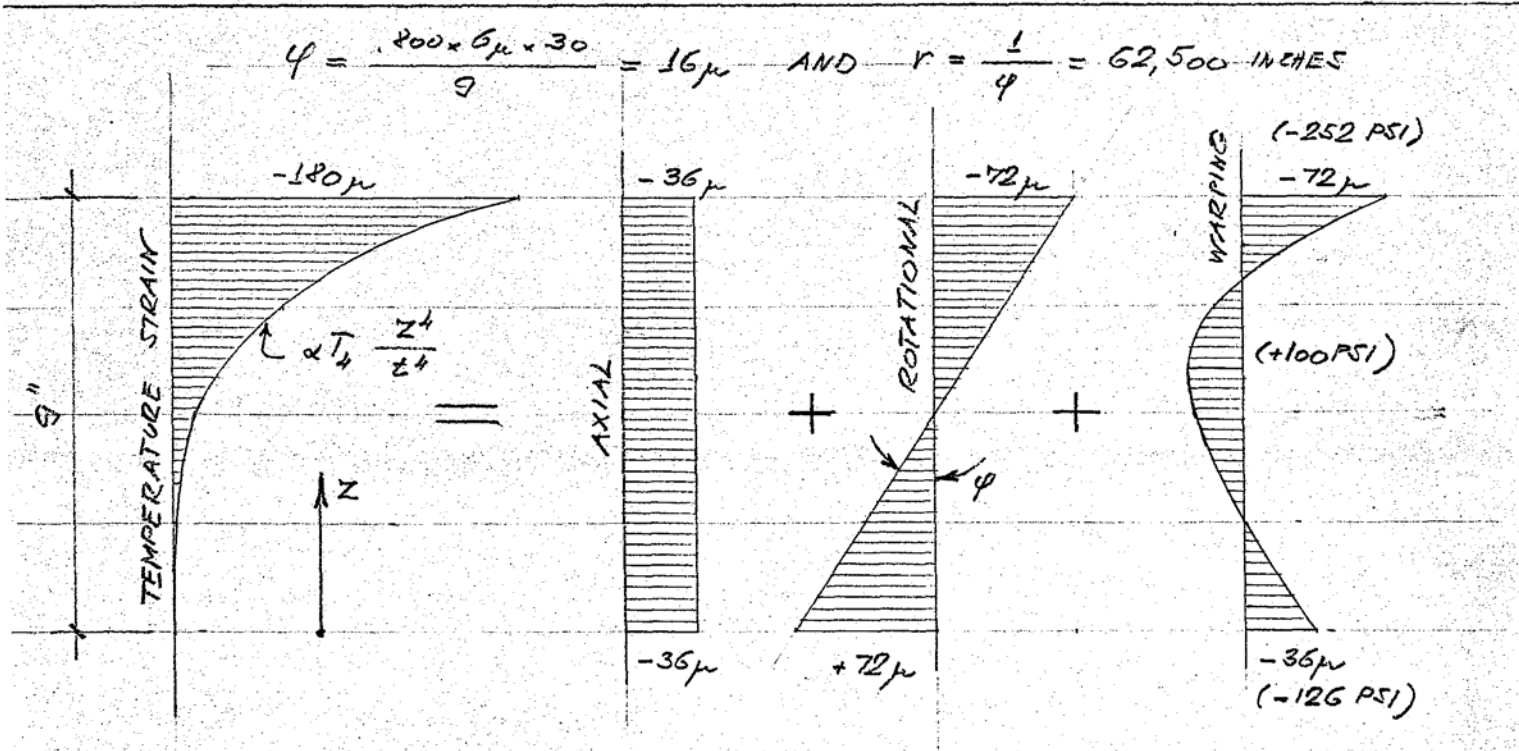

BREAKDOWN OF TEMPERATURE STRAINS

Figure 2

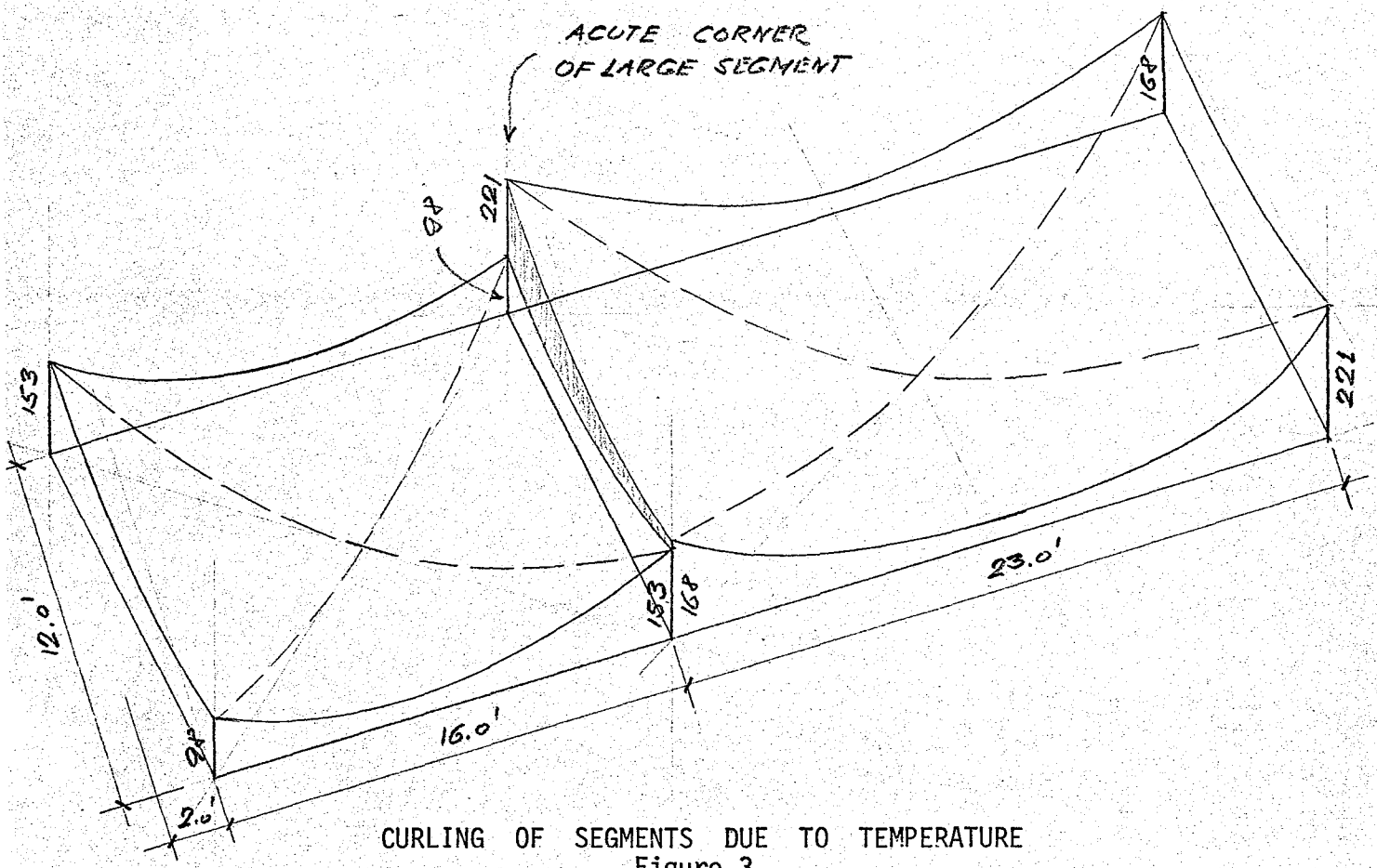

CURLING OF SEGMENTS DUE TO TEMPERATURE
Figure 3

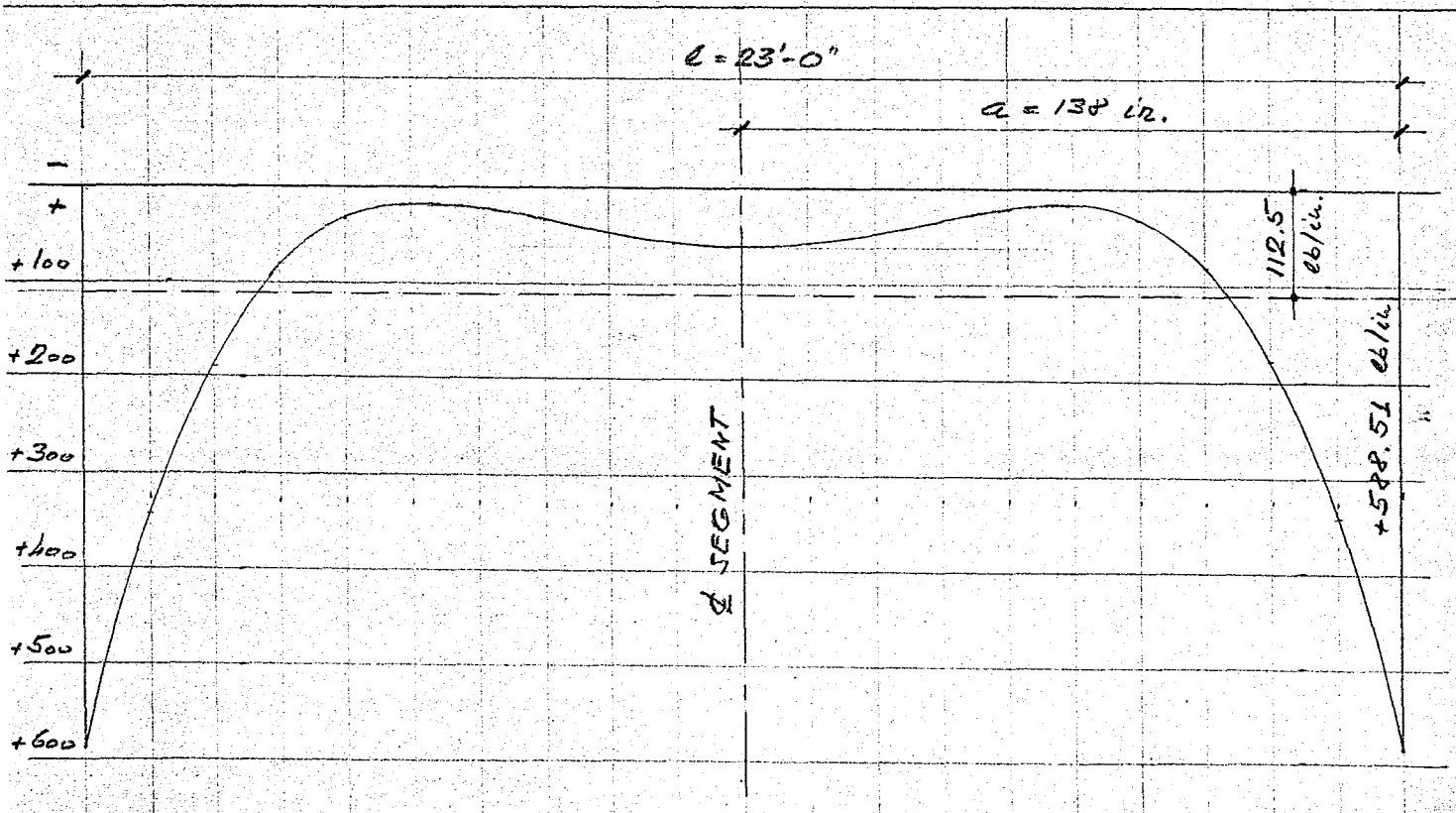

TEMPERATURE DEFLECTION OF A 23.0 FT. LONG SEGMENT
Figure 4

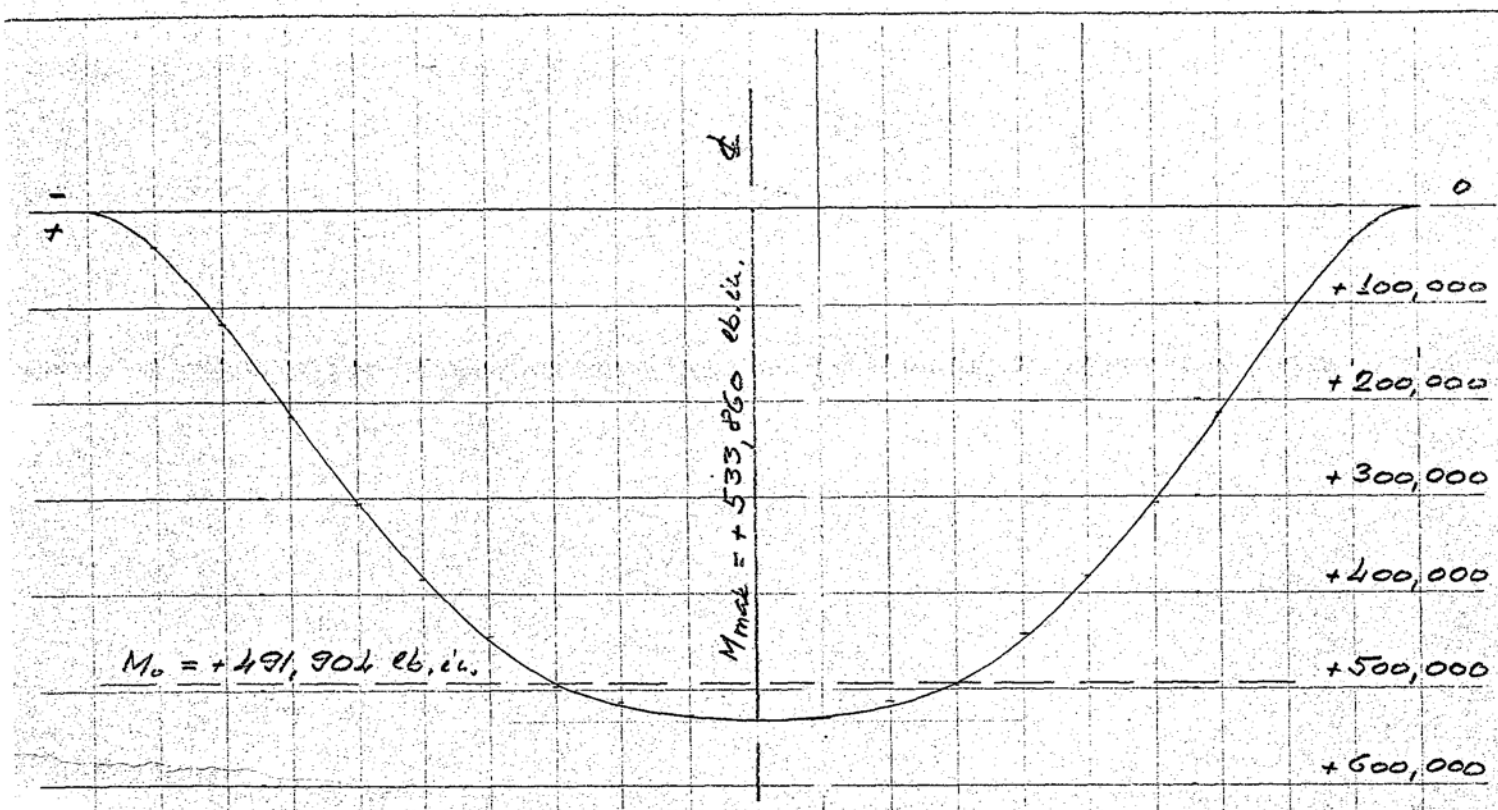

MOMENT DUE TO TEMPERATURE

Figure 5

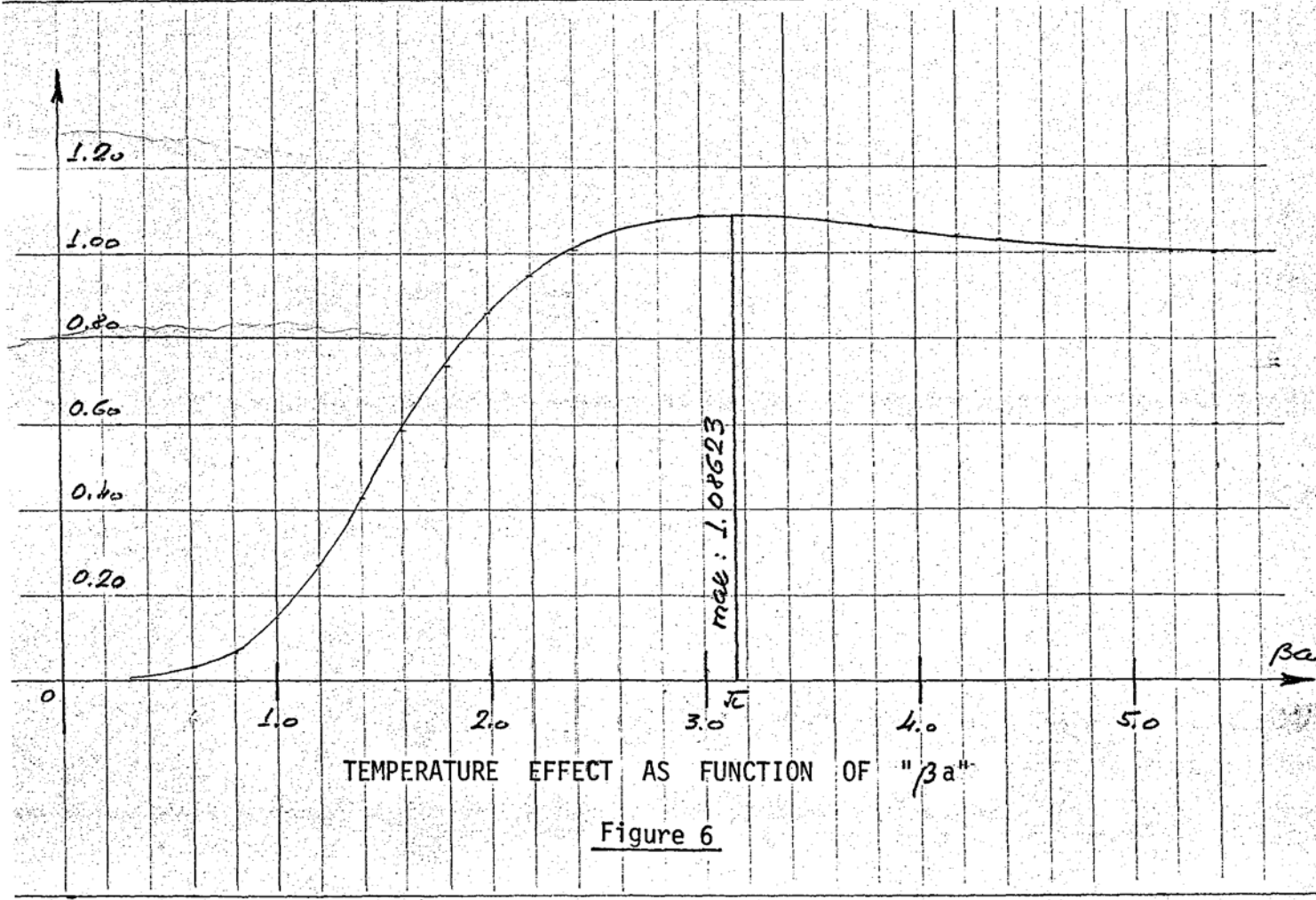

TEMPERATURE EFFECT AS FUNCTION OF "βa"

Figure 6

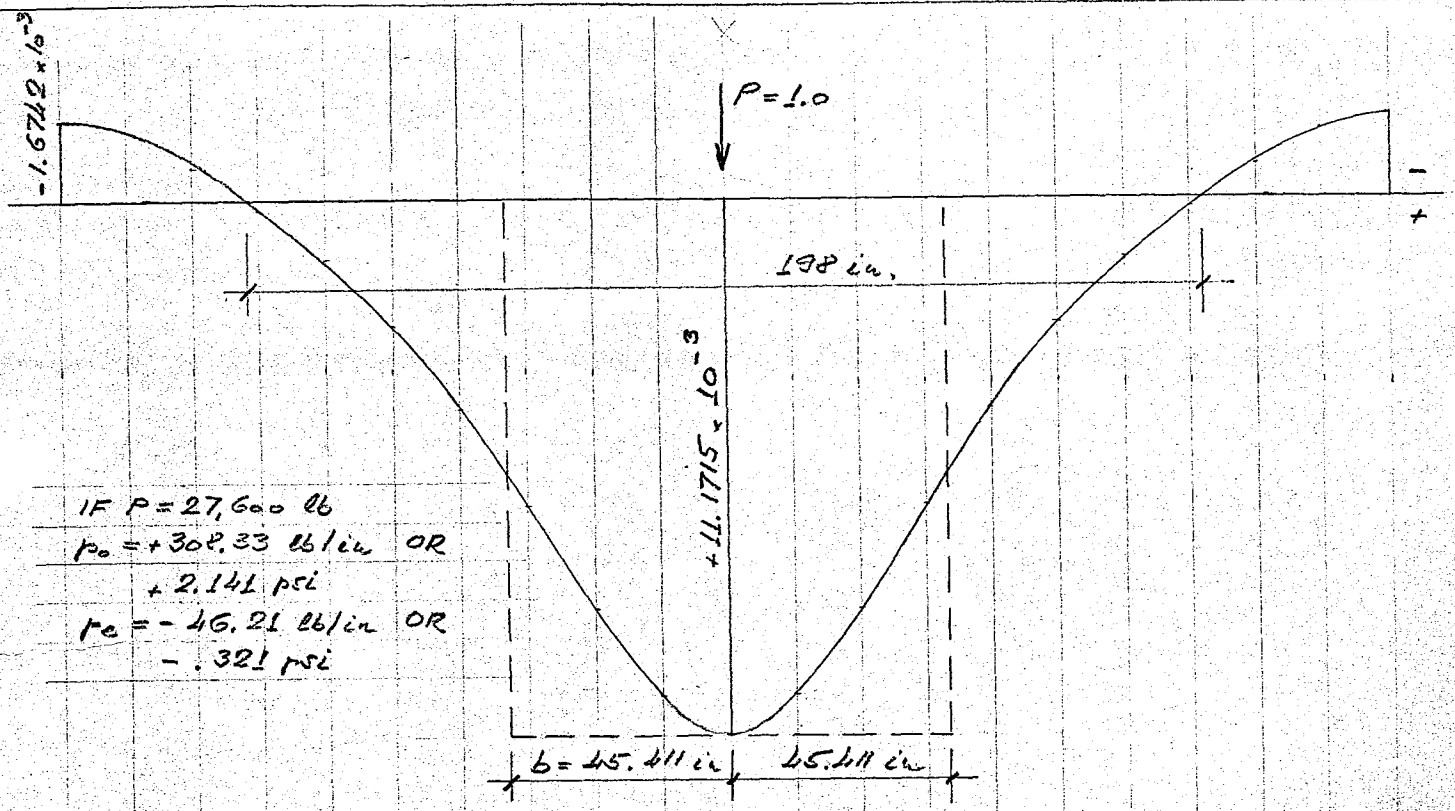

DEFLECTION UNDER CENTRAL POINT LOAD
FIGURE 7

MOMENTS DUE TO COMBINED EFFECTS
FIGURE 11

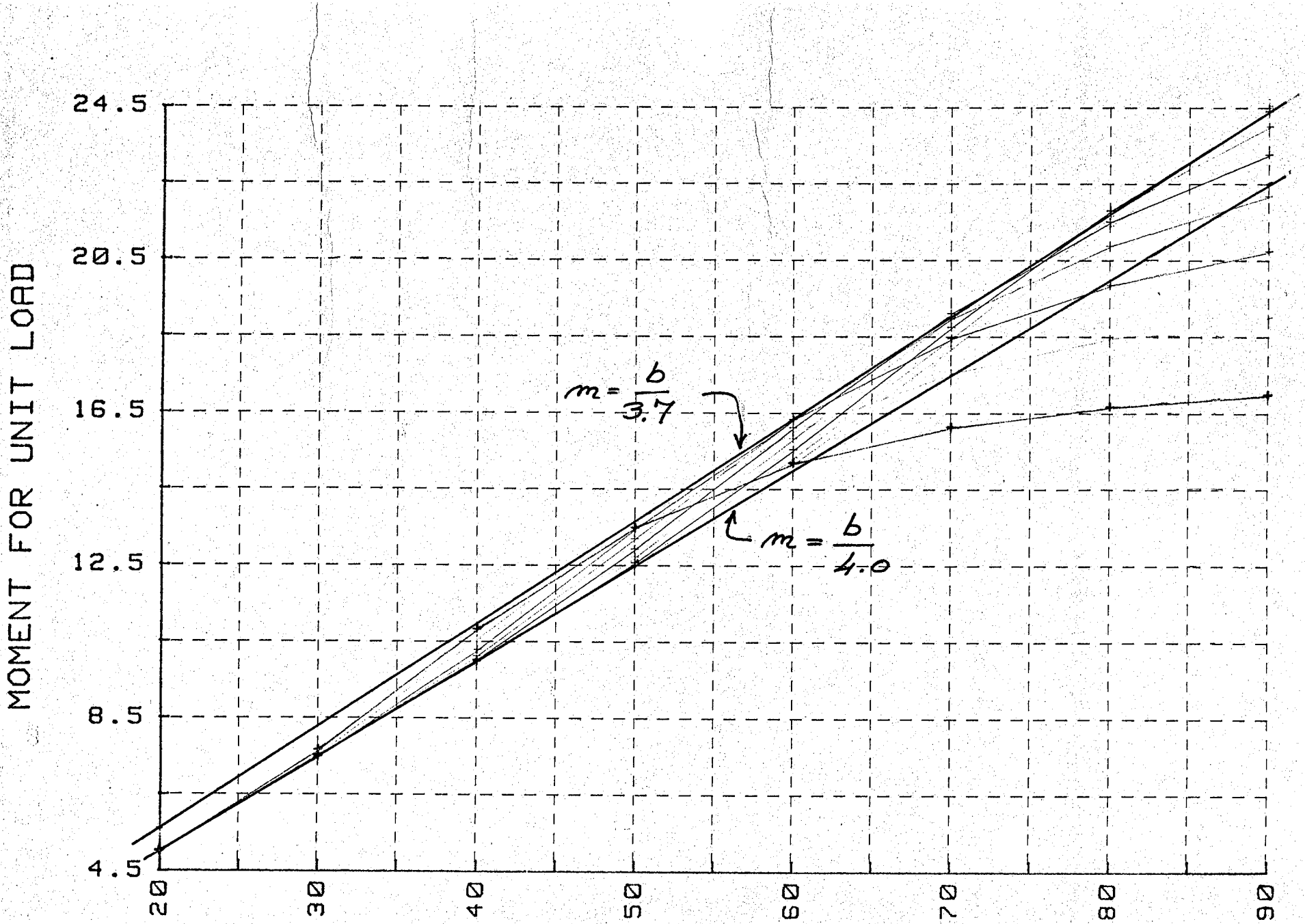

MOMENTS UNDER CENTRAL POINT LOAD

Figure 8

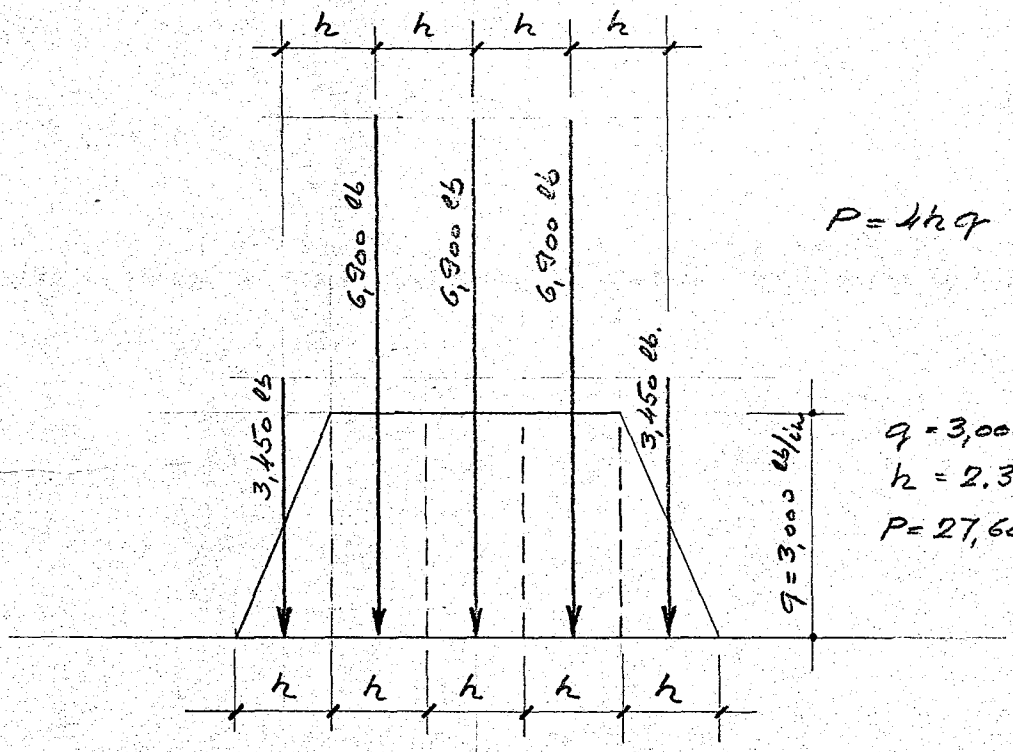

PATCH DISTRIBUTION OF AXLE WEIGHT
FIGURE 9

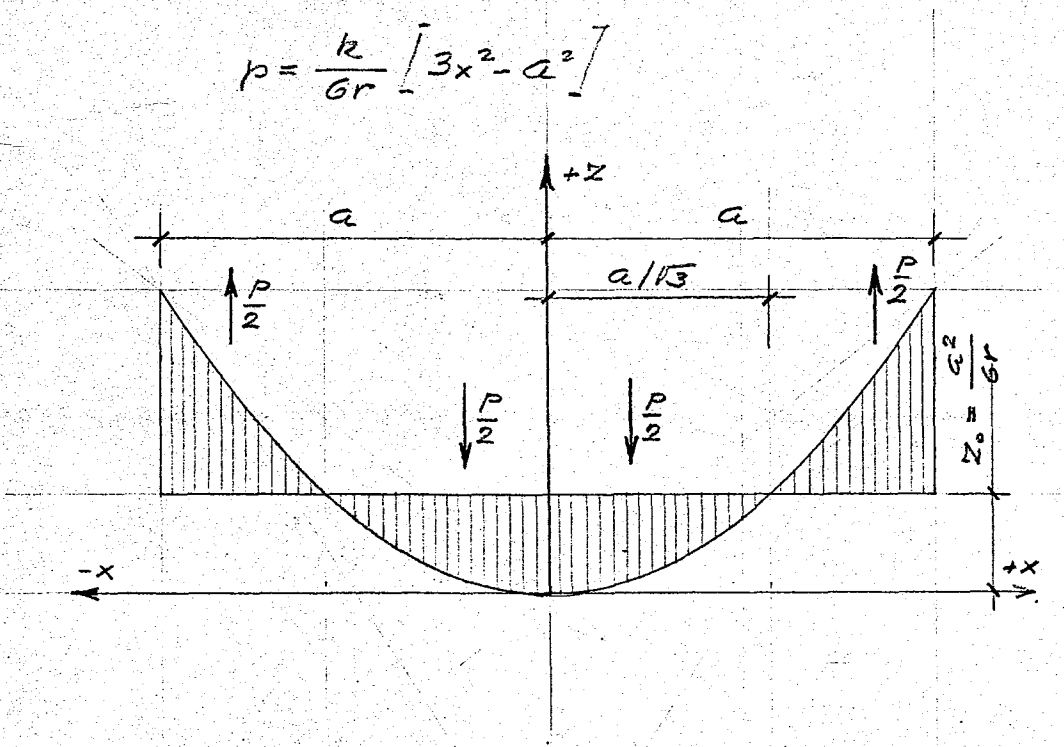

VIRTUAL TEMPERATURE LOAD
FIGURE 12

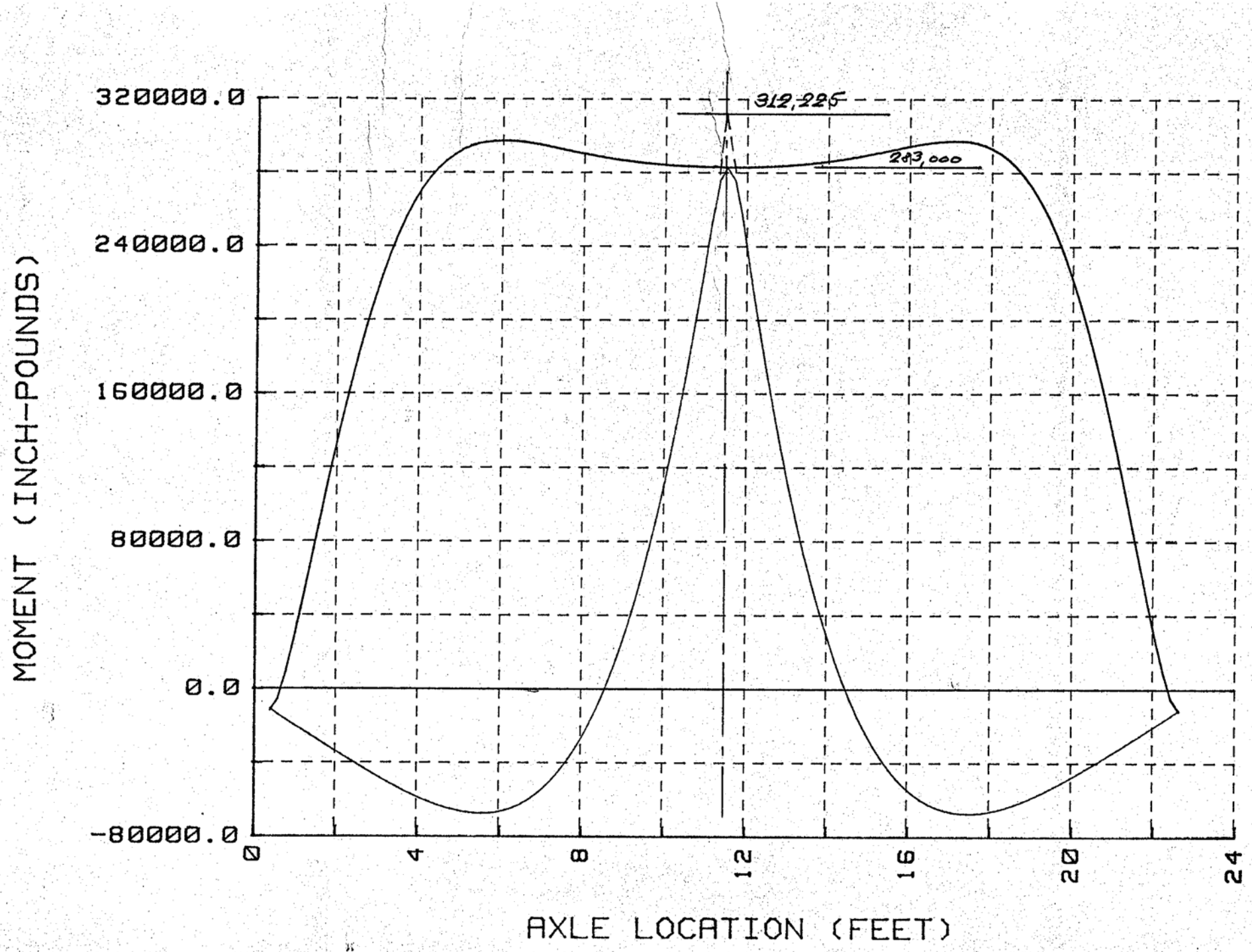

MOMENTS DUE TO AXLE LOAD

FIGURE 10

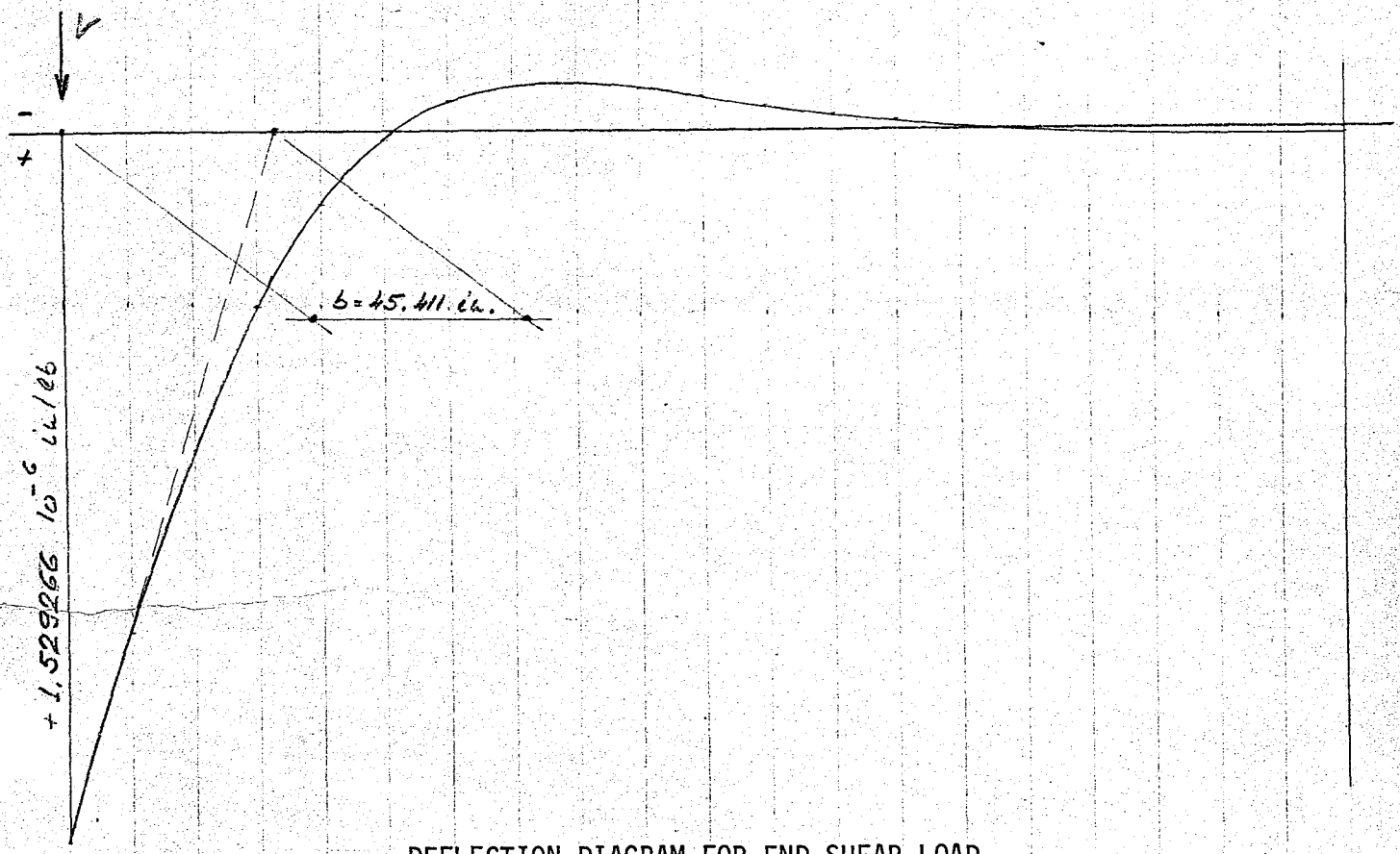

DEFLECTION DIAGRAM FOR END SHEAR LOAD
FIGURE 13

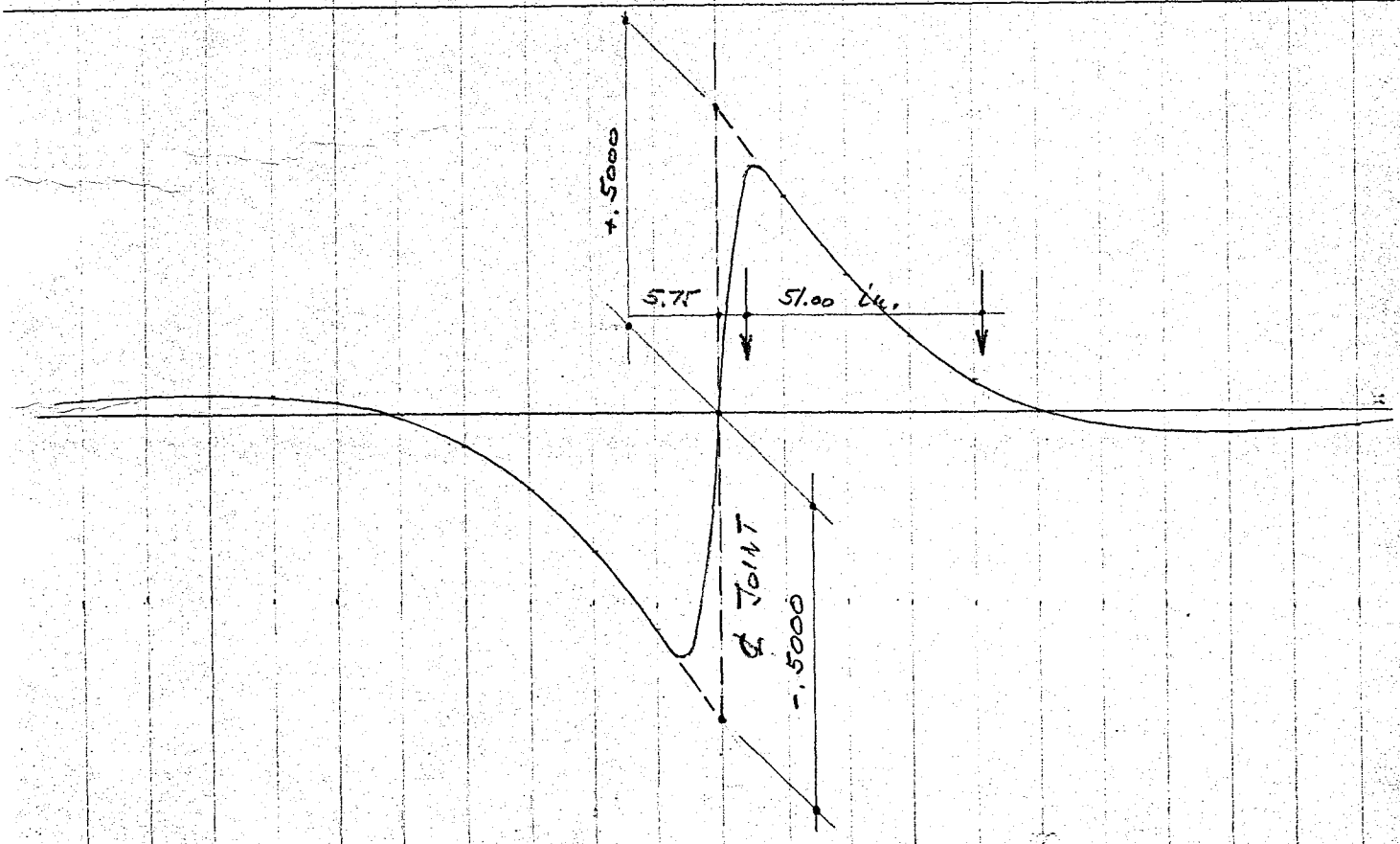

SHEAR FORCE INFLUENCE LINE
FIGURE 14

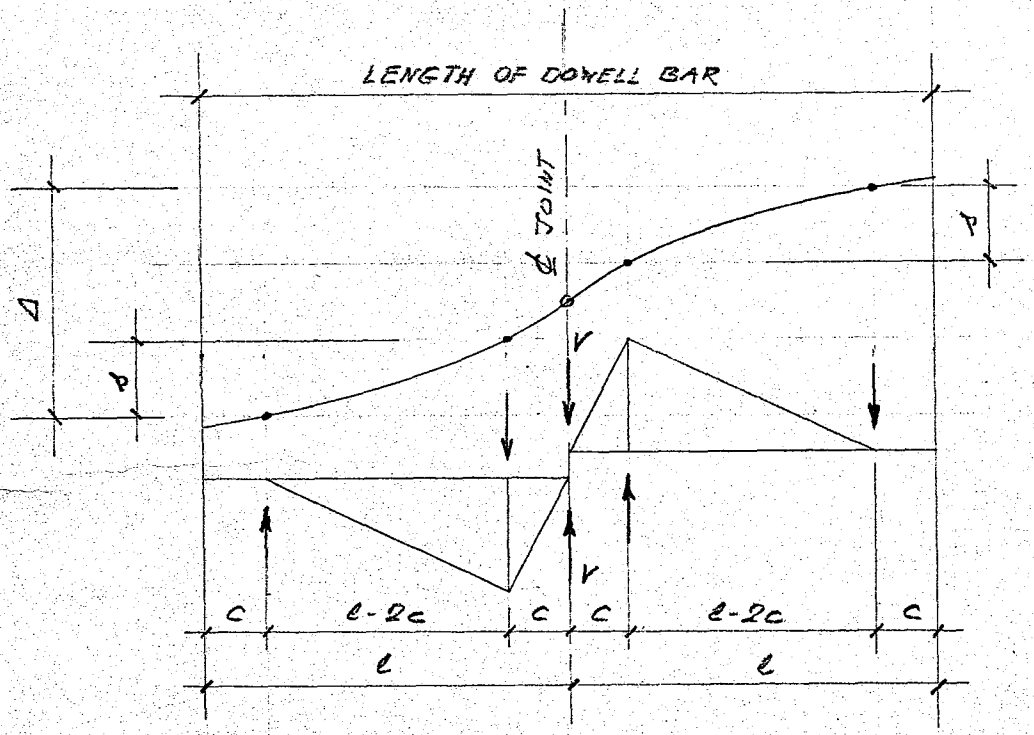

PERFORMANCE CHARACTERISTICS OF DOWELS
FIGURE 15

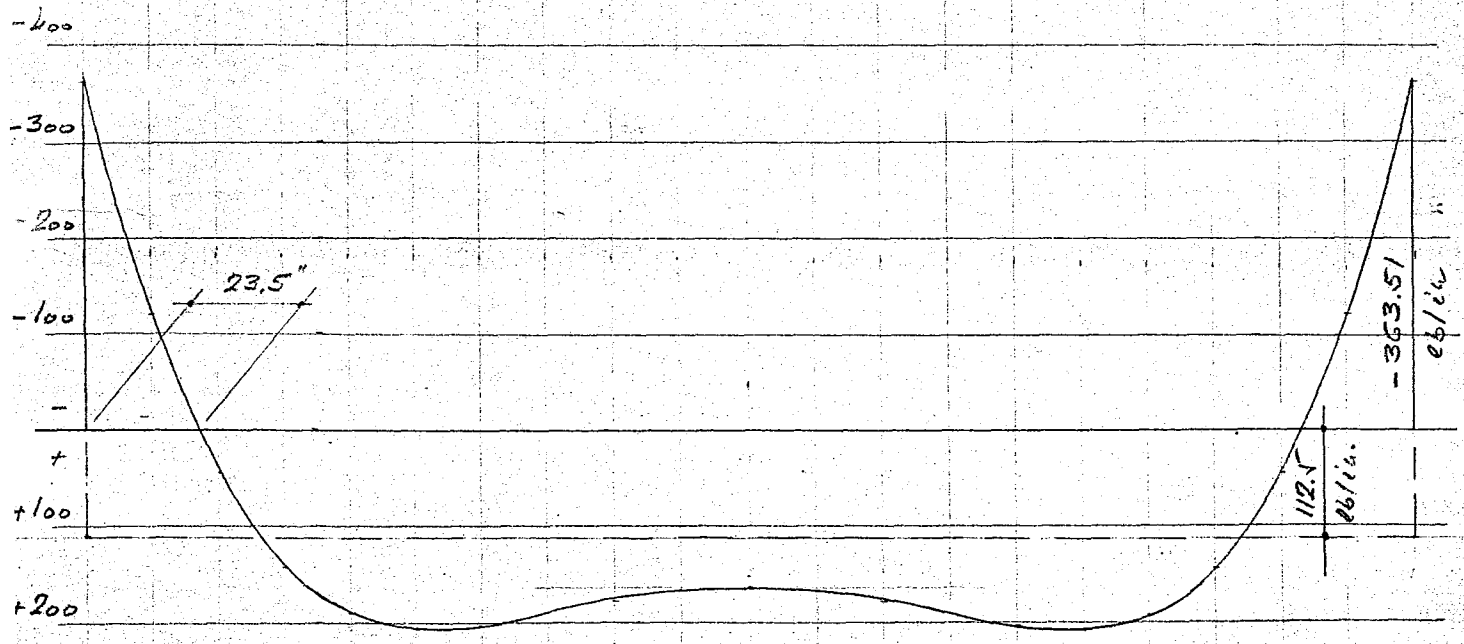

CURLING DUE TO TEMPERATURE WITH FULL SUPPORT
FIGURE 16

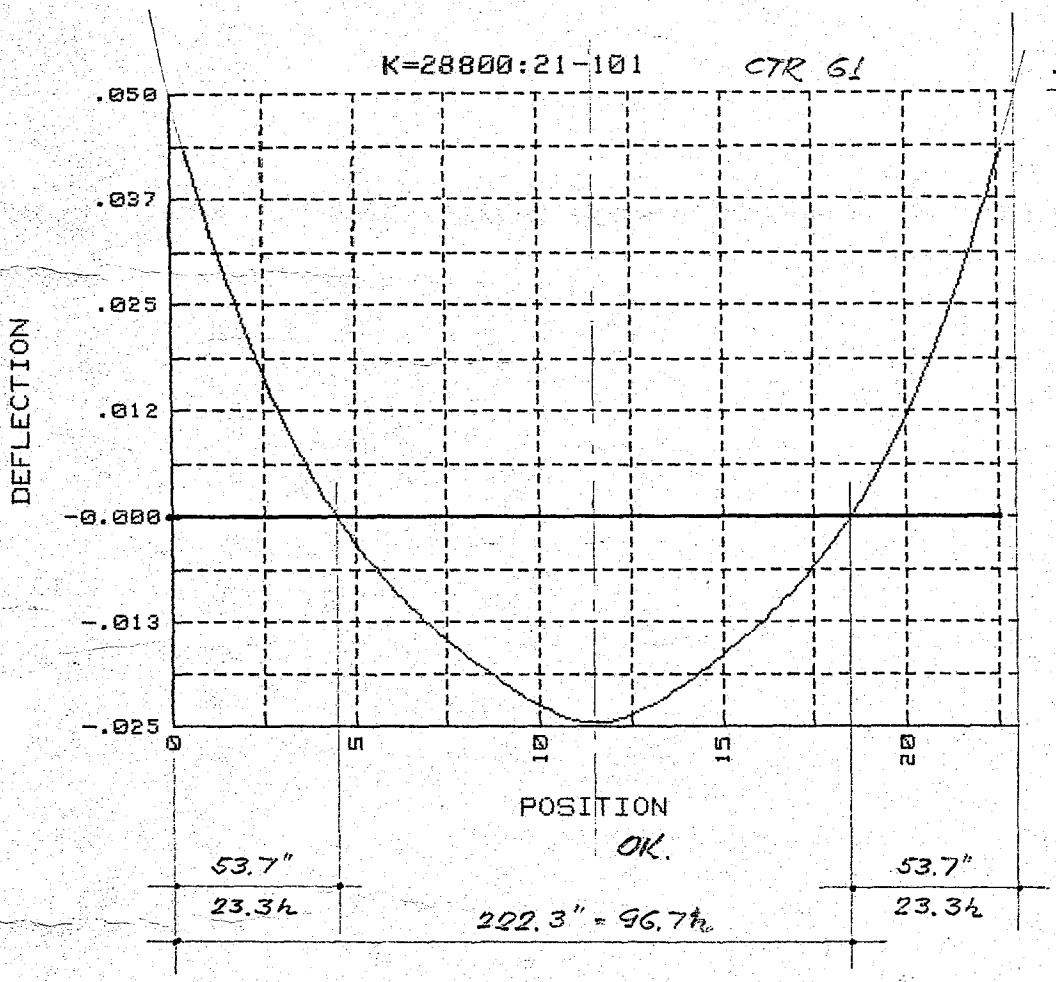

CURLING DUE TO TEMPERATURE WITH PARTIAL SUPPORT
FIGURE 17

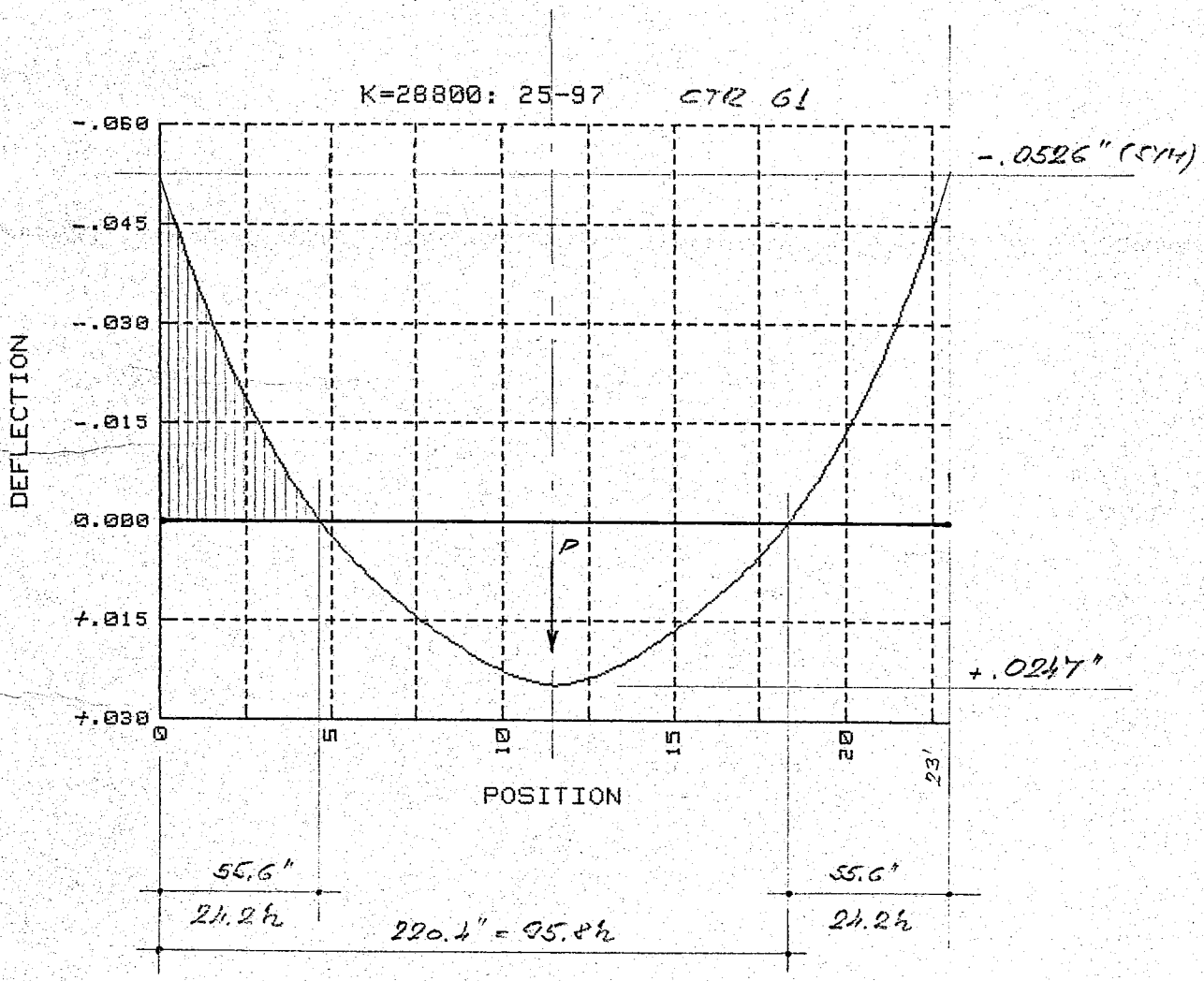

EFFECT OF A MOVING AXLE LOAD
FIGURE 18a

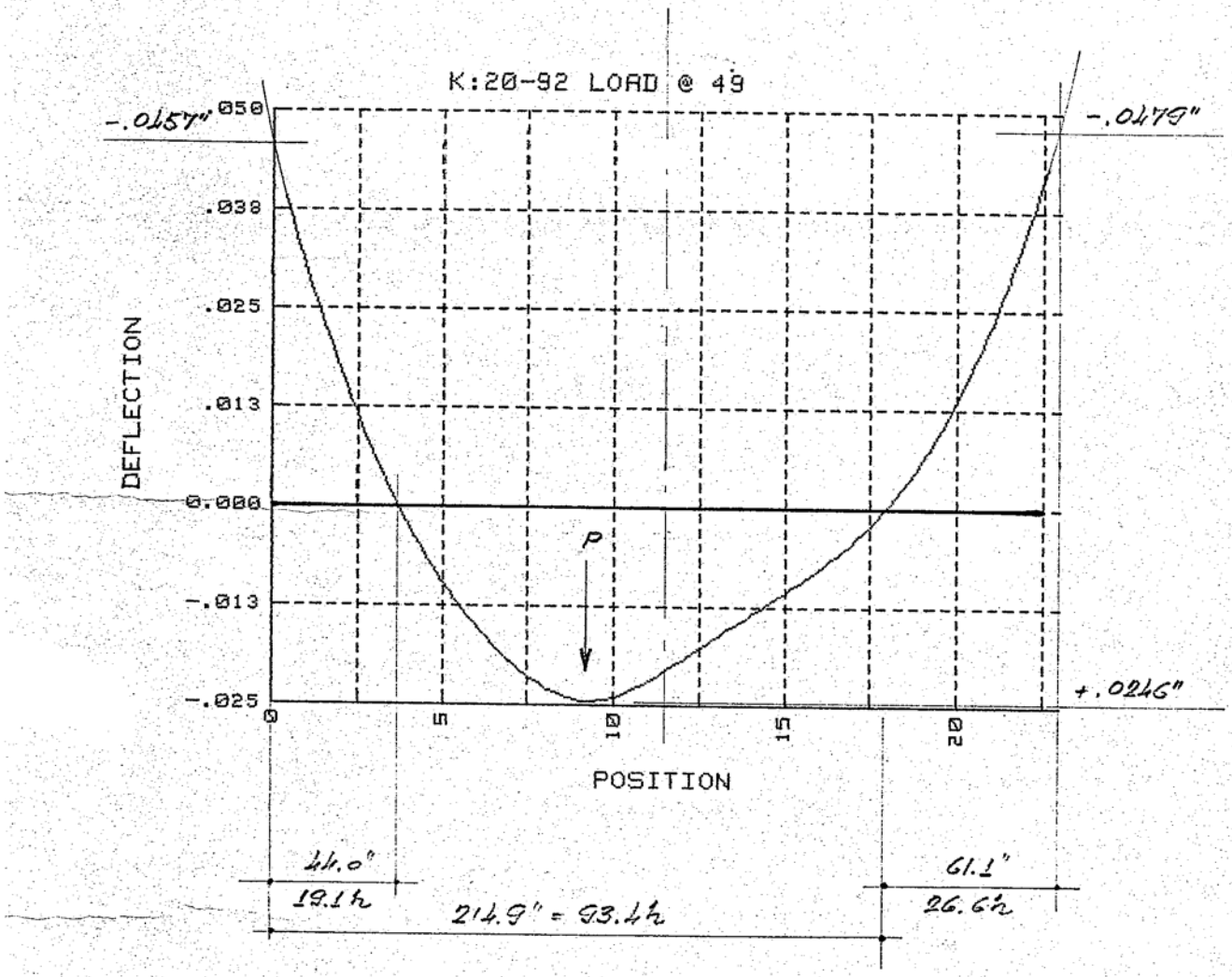
K:20-92 LOAD @ 49
-.0157"
-.0479"
.050
.038
.025
.013
0.000
-.013
-.025
DEFLECTION
P
+.0246"
0
5
10
15
20
POSITION
44.0"
19.1h
214.9" = 93.4h
61.1"
26.6h

FIGURE 18b

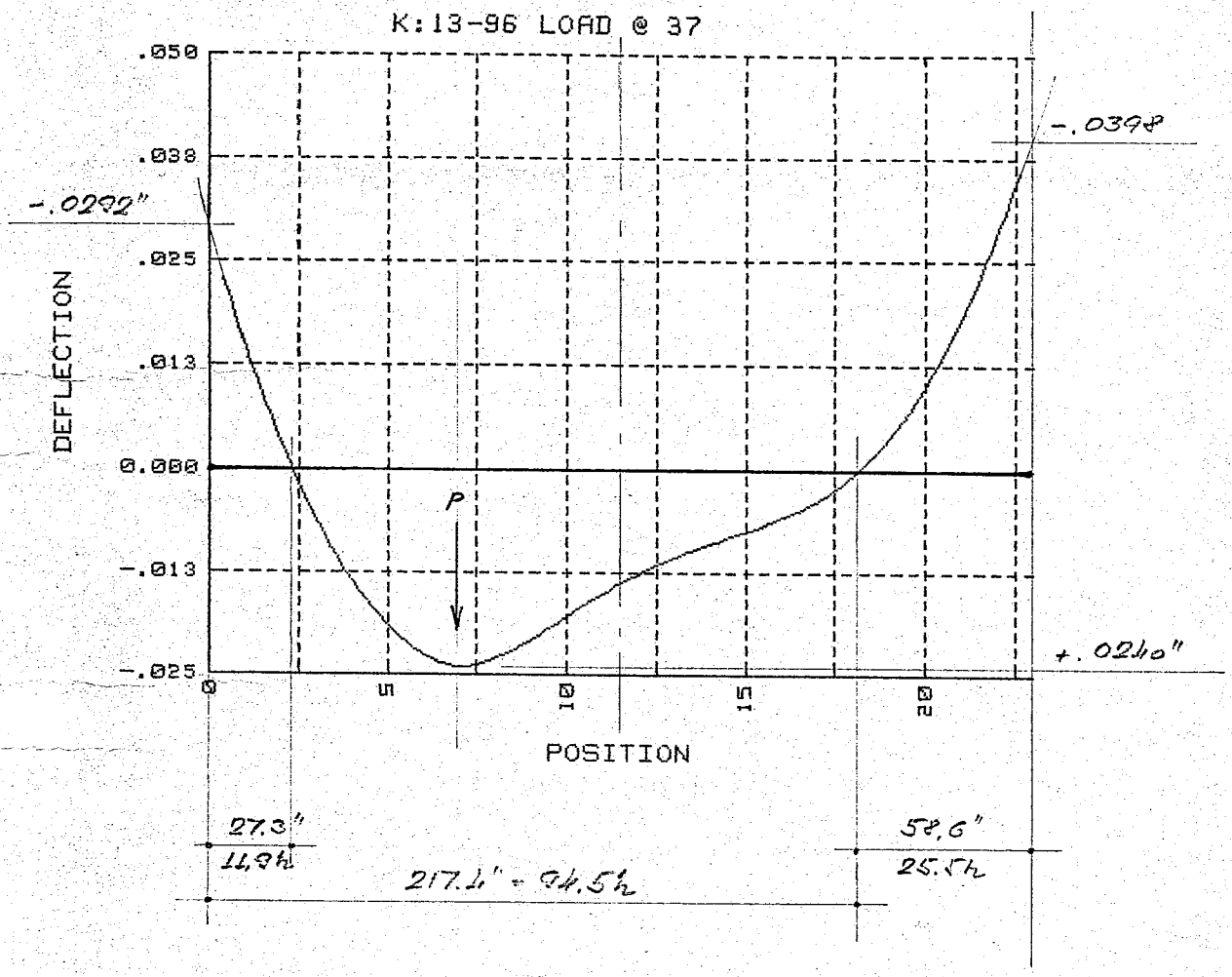
K:13-96 LOAD @ 37
.050
.038
.025
.013
0.000
-.013
-.025
DEFLECTION
-.0292"
-.0398
+.0240"
P
0
5
10
15
20
POSITION
27.3"
11.9h
58.6"
25.5h
217.1" = 94.5h

FIGURE 18c

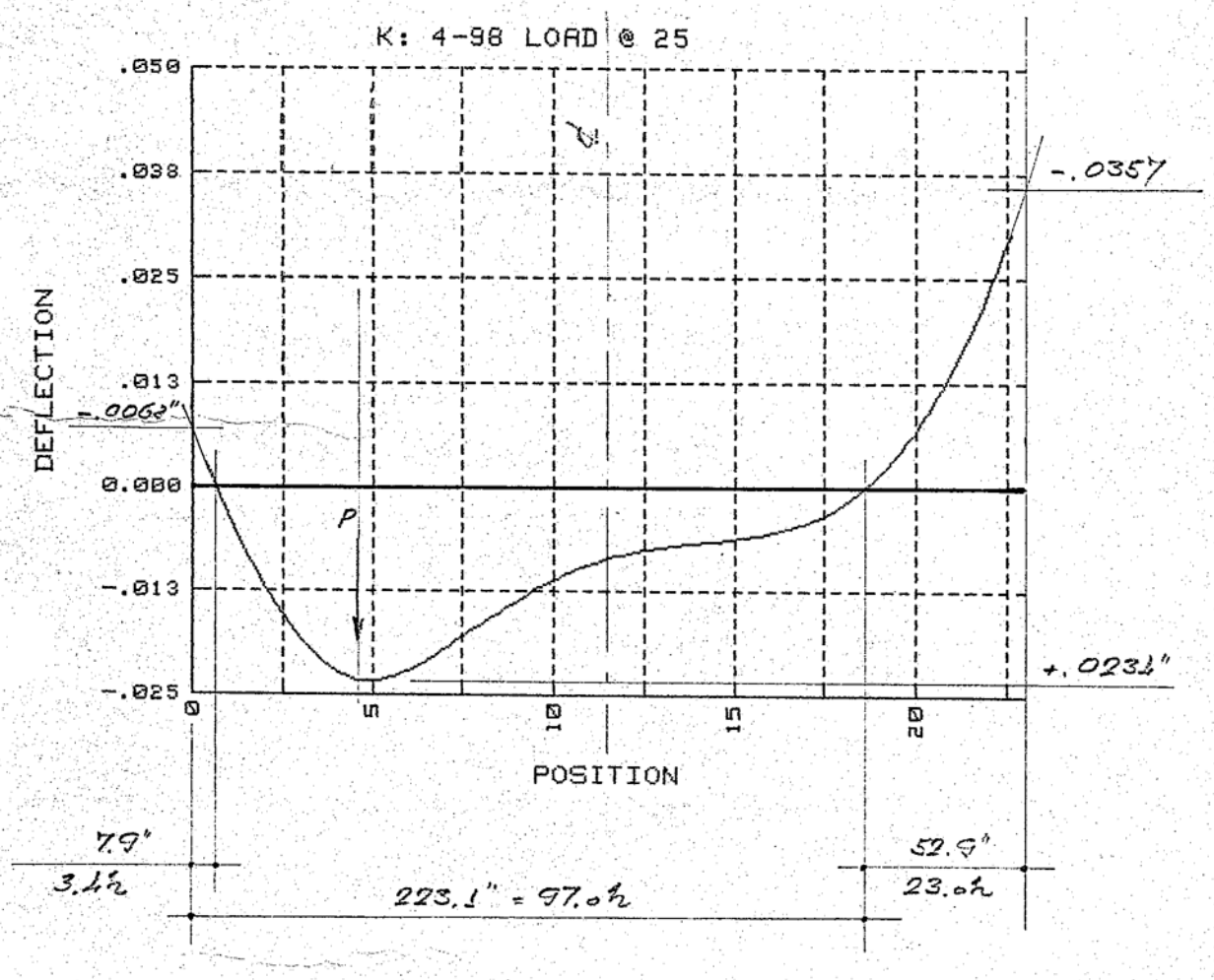
K: 4-98 LOAD @ 25
.050
.038
.025
.013
0.000
-.013
-.025
DEFLECTION
-.0062"
-.0357
+.0234"
P
0
5
10
15
20
POSITION
7.9"
3.1h
223.1" = 97.0h
52.9"
23.0h

FIGURE 18d

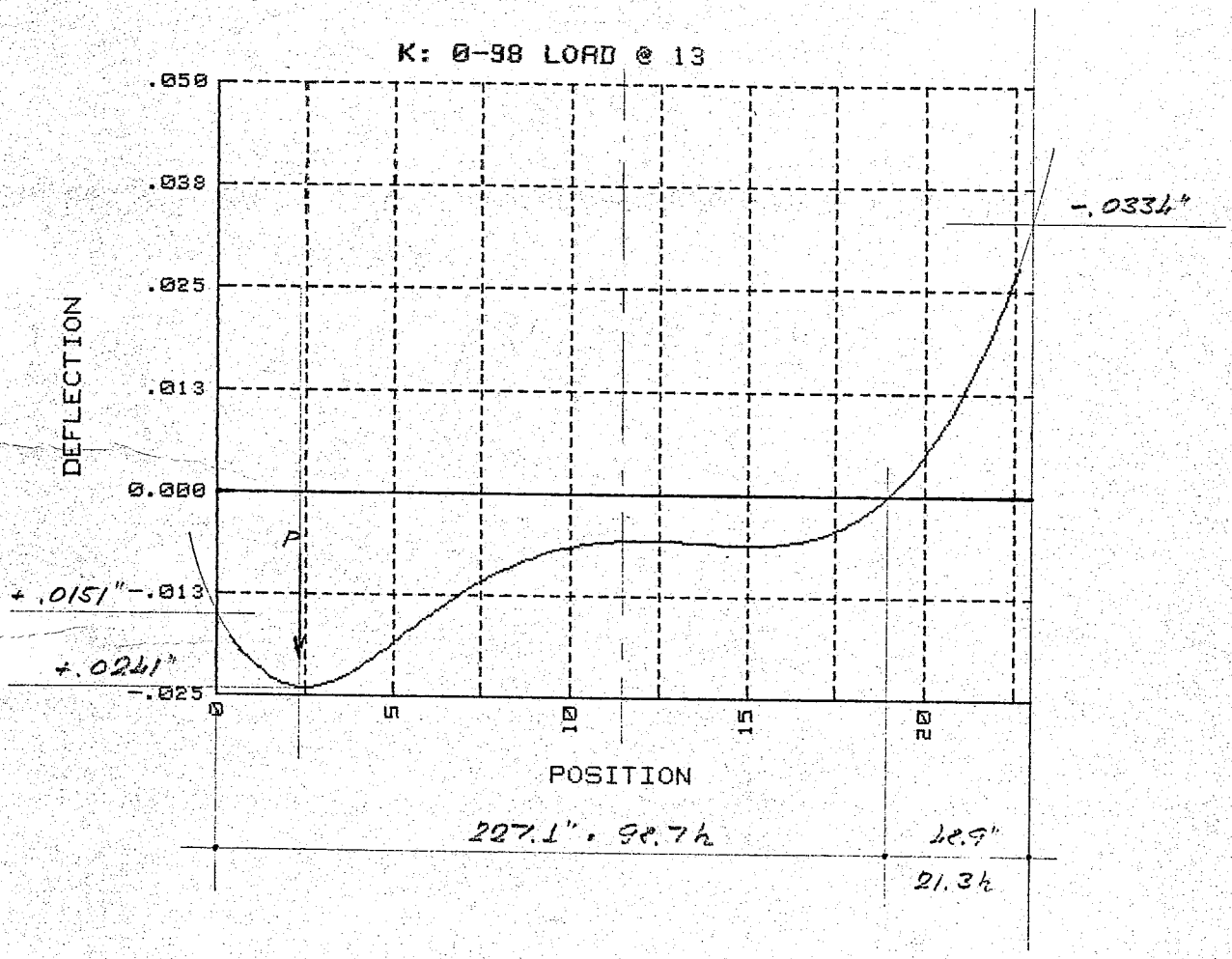
K: 0-98 LORD @ 13
.050
.038
.025
.013
0.000
-.025
DEFLECTION
P
+.0151"
-.013
+.0241"
-.0334"
0
5
10
15
20
POSITION
227.1", 98.7k
18.9"
21.3k

FIGURE 18c

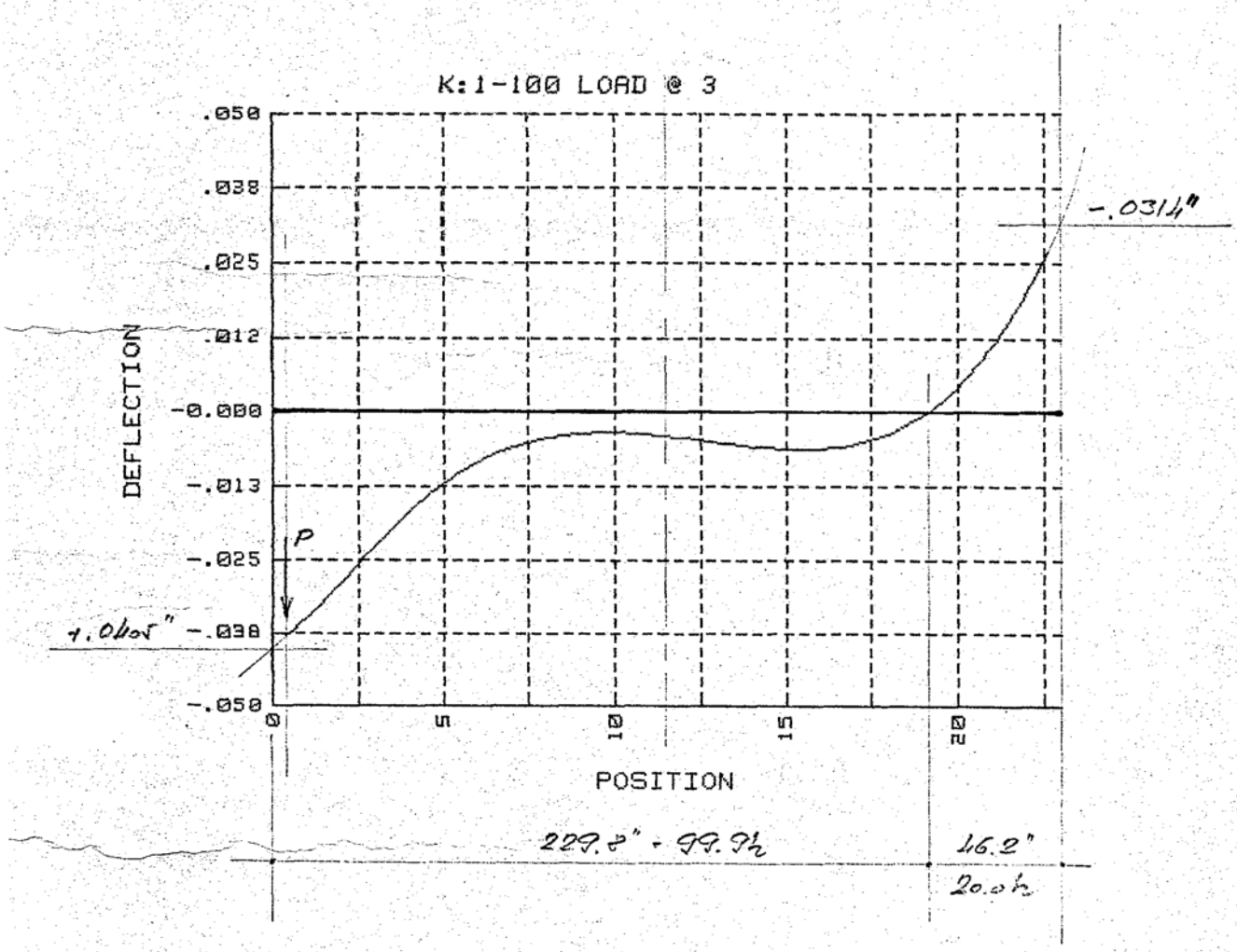
K:1-100 LOAD @ 3
.050
.038
.025
.012
-0.000
-.013
-.025
-.038
-.050
DEFLECTION
P
-.0314"
1.0625" -.038
0
5
10
15
20
POSITION
229.8" - 99.9%
46.2"
20.0%

FIGURE 18f

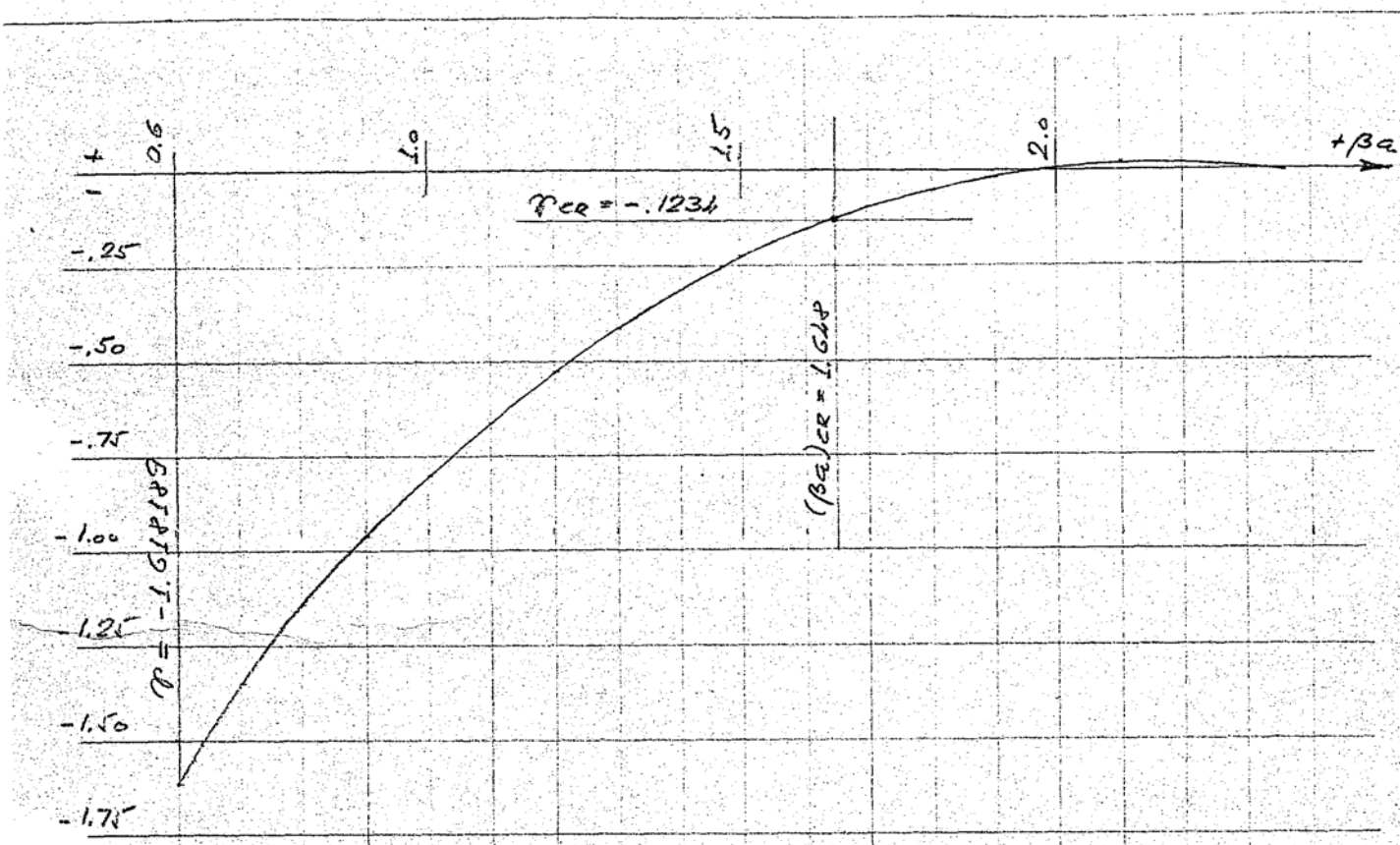

CRITICAL MINIMUM LENGTH OF SEGMENT
FIGURE 19

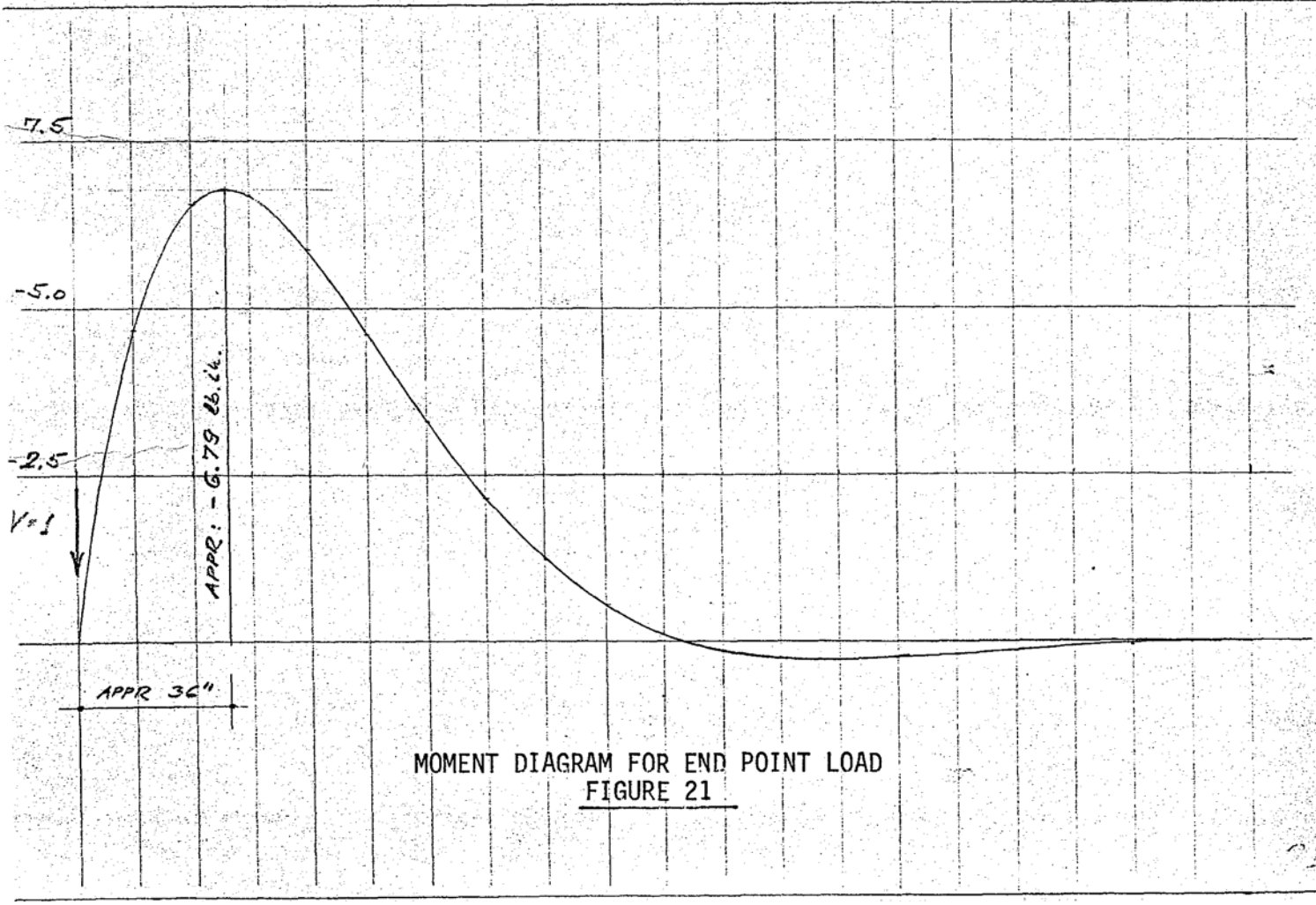

MOMENT DIAGRAM FOR END POINT LOAD
FIGURE 21

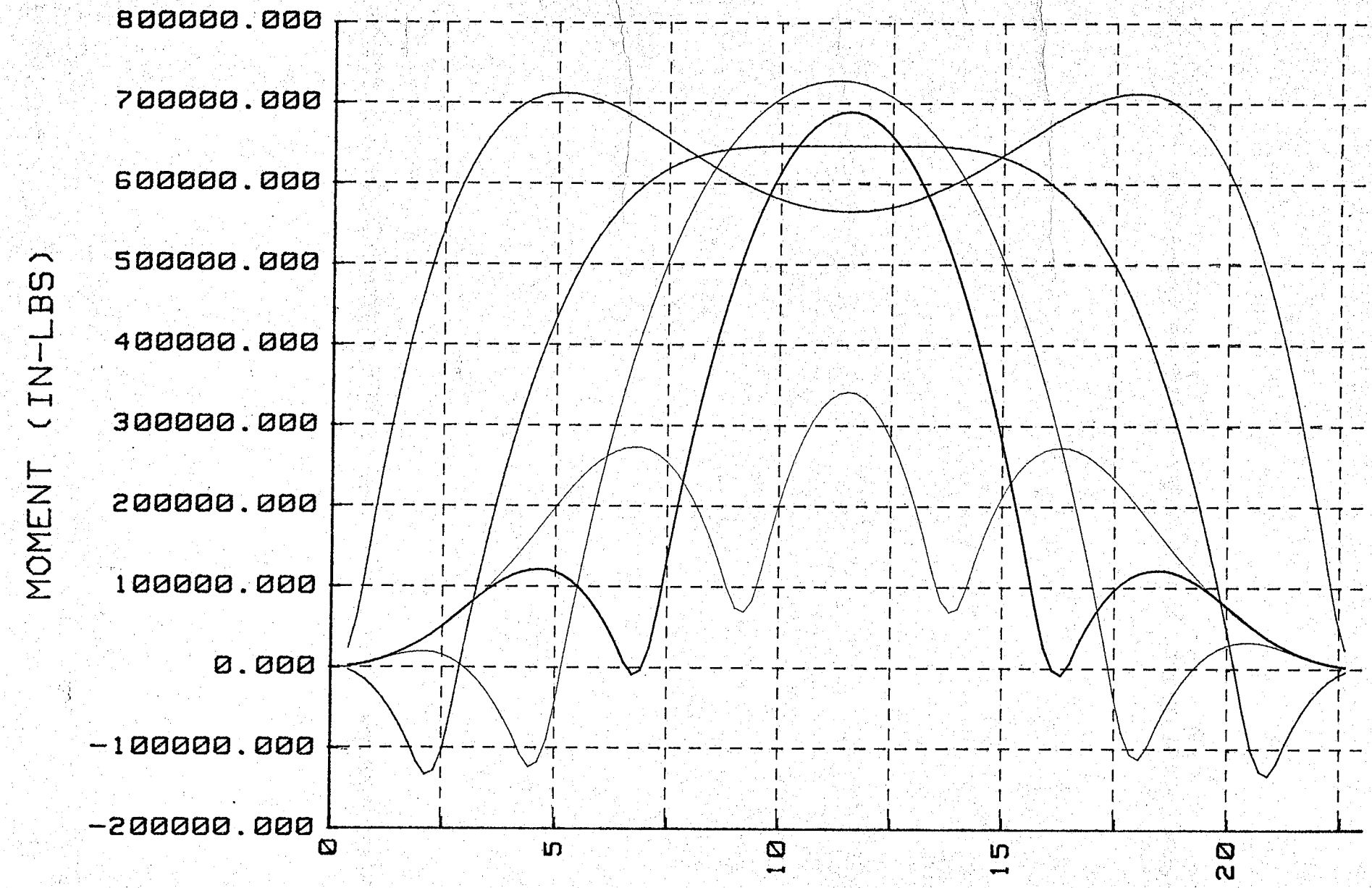

MAXIMUM NEGATIVE MOMENTS

Figure 20